to that seen for the ethylene complex. The titanium–methyl LMO (Figure 7b), however, shows the new bonding interactin between C_2 and C_7. This interaction may be loosely described as donation of the Ti–CH_3 bonding pair into the ethylene π^* orbital. The atomic populations and calculated hybridizations[36] for orbitals 6a, 6b, 7a, and 7b are presented in Table V. Clearly, d-orbital participation is very important in both the reactant and the transition state.

In the Introduction, symmetry arguments were presented to explain why the 2 + 2 reaction in Ziegler–Natta polymerization is not symmetry forbidden. To further illustrate this fact, wave-function plots and electron density plots for the two important bonding canonical molecular orbitals (the first two HOMO's) in the $Cp_2TiCH_3^+$ transition state are shown in Figure 8. As the symmetry analysis showed, we have two bonding orbitals in the transition state for this reaction. Plot 1a illustrates the bonding interaction between the ethylene carbons (C_1 and C_2) and the titanium, as well as the bonding interaction between the methyl carbon (C_7) and one of the ethylene carbons (C_2). In the second molecular orbital, 2a, we see bonding between the methyl carbon (C_7) and the titanium and C_1 and titanium. There is no interaction, however, between C_2 and C_7. This is further exemplified by the electron density plot, 2b, and supports the fact that the C_2–C_7 bond in the transition state has not fully formed yet.

(36) Switkes, E.; Stevens, R. M.; Lipscomb, W. N.; Newton, M. D. *J. Chem. Phys.* **1969**, *51*, 2085.

Conclusions

We have presented a full reaction profile for the direct insertion polymerization of ethylene by a real Ziegler–Natta initiator system, $Cp_2TiCH_3^+$. Geometries for the structures along the reaction pathway were optimized using the PRDDO method. Ab initio Hartree–Fock calculations with and without MP2 corrections were used to reevaluate the energetics of these structures. The activation energy at the MP2 level of theory is +9.8 kcal/mol for the $Cp_2TiCH_3^+$ system. The binding energy of ethylene was found to be 15.9 kcal/mol for the $Cp_2TiCH_3^+$ initiator, while the overall ΔE for the insertion process is −12.4 kcal/mol.

The results of this study indicate that direct insertion without alkyl-aluminum assistance and without agostic interactions is indeed a viable mechanism for the Ziegler–Natta polymerization of ethylene using a titanium-based initiator system.

Finally, this work indicates that the substitution of chlorines for cyclopentadienyl ligands in theoretical studies on organometallic complexes must be done with caution. While the calculated transition states and overall exothermicities for the two reactions studied are fairly similar, the ethylene binding energies are significantly different.

Acknowledgment. We thank the Robert A. Welch Foundation (Grant Y-743) and Cray Research, Inc., for support and the University of Texas Center for High Performance Computing for computing time.

Photochemistry in a Box. Photochemical Reactions of Molecules Entrapped in Crystal Lattices: Mechanistic and Exploratory Organic Photochemistry[1,2]

Howard E. Zimmerman* and Michael J. Zuraw

Contribution from the Department of Chemistry, University of Wisconsin, Madison, Wisconsin 53706. *Received March 29, 1989*

Abstract: An exploration was made of the photochemical behavior in the crystalline state of a series of molecules we have previously studied in solution. The reactions studied fall into the categories of cyclohexenone rearrangements, reactions of di-π-methane systems, and the behavior of a molecule giving a long-range phenyl migration in solution. The 4,4-diarylcyclohexenones differed from the solution behavior in giving the trans-bicyclic photoproducts without the cis isomers and the 3,4-diarylcyclohexenones. In the case of 4,5,5-triphenylcyclohexenone, the bicyclic photoproduct had inverted stereochemistry compared with solution and otherwise showed entirely different photochemistry than the usual solution cyclobutanone formation. The di-π-methane systems gave rise to three types of behavior: (1) An intramolecular $2_\pi + 2_\pi$ cycloaddition between a dicyanovinyl and a phenyl group, (2) di-π-methane reactivity but with reversed regioselectivity, and (3) cyclopentene formation where the reactant has an additional vinyl group on the methane carbon. Finally, 1,1,5,5-tetraphenyl-3,3-dimethyl-1-penten-5-ol afforded five- and six-membered ring ethers rather than the solution phenyl migration. Solid-state quantum yields were determined with use of a newly designed apparatus. Several quantitative approaches for correlating solid-state reactivity to molecular geometry and crystalline constraints were devised.

For several decades our research group has pursued the investigation of solution photochemistry with an aim of encountering new organic transformations, determining the corresponding reaction mechanisms, and then correlating excited-state reactivity with structure. This reactivity was shown to be controlled by various intramolecular factors such as excited-state bond orders, electron densities, and hypersurface energy effects.[3]

However, organic photochemistry has included many studies of crystalline solids. The dimerization of crystalline cinnamic acid to the truxillic and truxinic acids was first studied at the beginning of the century.[4] With the advent of X-ray crystallography

(1) This is Paper 158 of our photochemical series and Paper 218 of our general series.

(2) For Paper 157 see: Zimmerman, H. E.; Cassel, J. M. *J. Org. Chem.*, **1989**, *54*, 3800–3816.

(3) (a) For some presentations of mechanistic treatments, note ref 3b–l. (b) Zimmerman, H. E., Seventeenth National Organic Symposium of the American Chemical Society, Bloomington, Indiana, 1961, pp 31–41. (c) Zimmerman, H. E.; Schuster, D. I. *J. Am. Chem. Soc.* **1961**, *83*, 4486–4487. (d) Zimmerman, H. E.; Schuster, D. I. *J. Am. Chem. Soc.* **1962**, *84*, 4527–4540. (e) Zimmerman, H. E. *Tetrahedron* **1963**, Suppl. 2, *19*, 393–401. (f) Zimmerman, H. E. In Advances in Photochemistry. Noyes, A., Jr., Hammond, G. S., Piits, J. N., Jr., Eds. *Interscience* **1963**, *1*, 183–208. (g) Zimmerman, H. E. *Science* **1966**, *153*, 837–844. (h) Zimmerman, H. E. *Angew. Chem., Int. Ed. Engl.* **1969**, *8*, 1–11. (i) Zimmerman, H. E.; Cutler, T. P. *J. Org. Chem.* **1978**, *43*, 3283–3303. (j) Zimmerman, H. E.; Factor, R. E. *Tetrahedron* **1981**, *37*, 125–141. (k) Zimmerman, H. E. *Acc. Chem. Res.* **1982**, *10*, 312–317.

0002-7863/89/1511-7974$01.50/0

Scheme I. Synthesis of Two Di-π-methane Systems

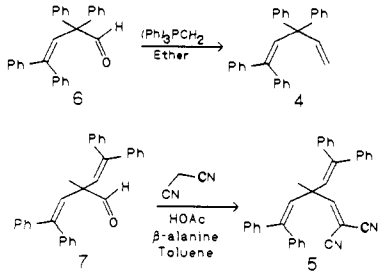

Schmidt and co-workers[5] were able to correlate reactivity with the proximity and orientation of reacting centers in photochemical dimerizations of alkenes. More recently, studies[6] have diversified to include a variety of photochemical reactions in the crystal. These are best exemplified by the elegant studies of Scheffer and co-workers.[7]

One conclusion from previous work is that proximity is a major factor in many solid-state photochemical processes.[8] Another suggested principle is least motion[9] wherein reactions involving the least molecular movement are favored. Finally, the concept of the "reaction cavity" has been proposed,[10] the idea being that a reaction will occur with a minimum of distortion of the reaction cavity.

Our studies began with the idea of investigating in crystalline medium the large variety of unimolecular rearrangements we had previously studied in solution.[3] One goal was the development of some further theoretical bases for prediction of reactivity in the crystal. The present study focussed attention on some of the more common photochemical reactions uncovered in our past efforts in the photochemistry of di-π-methane systems, cyclohexenones, and an unsaturated alcohol.

Results

Study of Di-π-methane Systems. Necessary Syntheses. Five di-π-methane systems were selected for study, namely **1–5**. The first three of these were known compounds with previously reported solution photochemistry while the last two had not previously been studied. The syntheses of di-π-methane systems **4** and **5** are outlined in Scheme I. In the case of tetraphenylpentadiene **4** the required aldehyde **6** was known from our previous studies.[11] For the synthesis of the tri-π-methane system **5**, the reactant aldehyde **7** was also known.[12]

Scheme II. Determination of Stereochemistry of Cyclopropanes **10**, **18**, and **17**

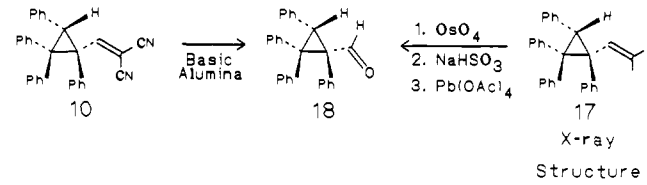

The Solution Photochemistry of the Di-π-methane Systems. The photochemistry of dienes **1–3** is outlined in eq 1, 2, and 3.[14,15]

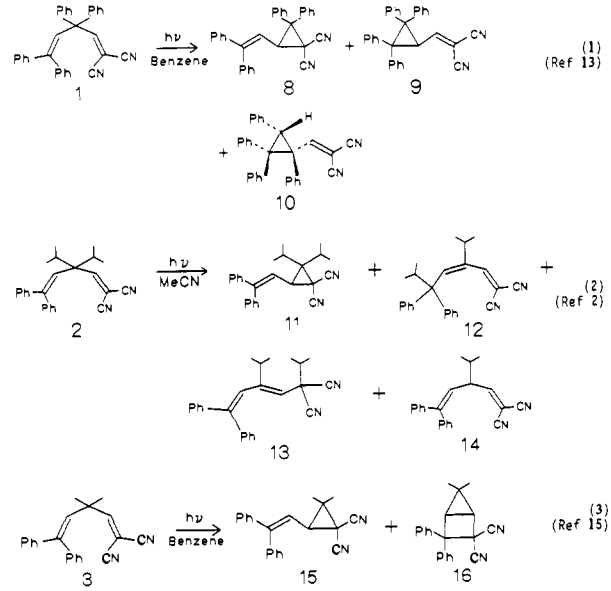

In the case of the tetraphenyldicyano diene **1**, three photoproducts were reported in our previous study. The first two of the three photoproducts (i.e. **8** and **9**) arise from a di-π-methane rearrangement involving vinyl–vinyl bridging. The last, **10**, results from phenyl–vinyl bridging. The present study used X-ray crystallography to establish the stereochemistry of the structurally related cyclopropane **17**.[11] In our earlier studies[11] the configuration of cyclopropyl aldehyde **18** was tentatively assigned by NMR analysis,[14] and this compound was interrelated to cyclopropane **10** as outlined in Scheme II.

We next turned to the solution photochemistry of tetraphenylpentadiene **4**. Two photoproducts, **19** and **20** (in a 1:1.3 ratio), resulted on direct irradiation, but only one compound, **19**, on sensitized irradiation. The structures of **19** and **20** were established by ozonolysis to the known[11] aldehydes **21** and **18**, respectively, as shown in eq 4 and 5. Therefore the photochemical transformation may be depicted as in eq 6.

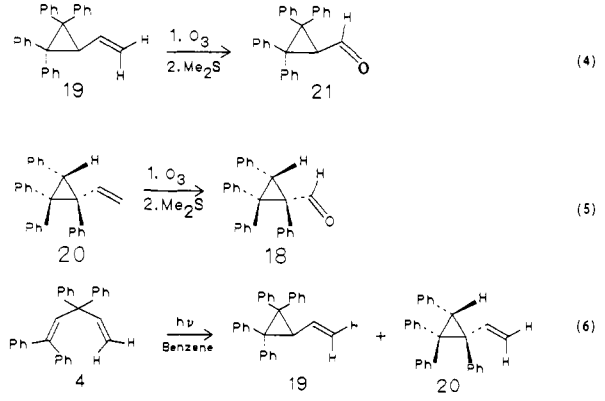

(4) (a) Bertram, J.; Kürsten, R. *J. Prakt. Chem.* **1895**, *51*, 323. (b) de Jong, A. W. K. *Chem. Ber.* **1923**, *56*, 818.

(5) Schmidt, G. M. J. *Solid State Photochemistry*; Ginsberg, D., Ed.; Verlag Chemie: New York, 1976.

(6) (a) Scheffer, J. R.; Garcia-Garibay, M.; Nalamasa, O. In *Organic Photochemistry*; Padwa, A., Ed., Marcel Dekker: New York, 1987; Vol. 8, pp 249–347. (b) Ramamurthy, V.; Venkatesan, K. *Chem. Rev.* **1987**, *87*, 433–481. (c) Desiraju, G. R., Ed. *Organic Solid State Chemistry*; Elsevier: Amsterdam, 1987. (d) Green, B. S.; Arad-Yellin, R.; Cohen, M. D. In *Topics in Stereochemistry*; Eliel, E. L., Wilen, S. H., Allinger, N. L., Eds.; Wiley: New York, 1986; Vol. 16, pp 131–218. (e) McBride, J. M.; Segmuller, B. E.; Hollingsworth, M. D.; Mills, D. E.; Weber, B. A. *Science* **1986**, *234*, 830–835.

(7) (a) Scheffer, J. R.; Ariel, S.; Evans, S. V.; Garcia-Garibay, M.; Harkness, B. R.; Omkaram, N.; Trotter, J. *J. Am. Chem. Soc.* **1988**, *110*, 5591–5592. (b) Scheffer, J. R.; Trotter, J.; Garcia-Garibay, M.; Wireko, F. *Mol. Cryst. Liq. Cryst. Inc. Nonlin. Opt.* **1988**, *156*, 63–84.

(8) (a) For olefin dimerizations: Gnanaguru, K.; Ramasubbu, N.; Venkatesan, K.; Ramamurthy, V. *J. Org. Chem.* **1985**, *50*, 2337–2346. (b) For hydrogen abstractions: Scheffer, J. R.; Trotter, J. *Rev. Chem. Intermed.* **1988**, *9*, 271–305.

(9) Cohen, M. D.; Schmidt, G. M. J. *J. Chem. Soc.* **1964**, 1996–2000.

(10) (a) Cohen, M. D. *Angew. Chem., Int. Ed. Engl.* **1975**, *14*, 386–393. (b) Some departures from least motion have been found.[6e,10c] (c) Chang, H. C.; Popovitz-Biro, R.; Lahav, M.; Leiserowitz, L. *J. Am. Chem. Soc.* **1987**, *109*, 3883–3893.

(11) Zimmerman, H. E.; Boettcher, R. J.; Braig, W. *J. Am. Chem. Soc.* **1973**, *95*, 2155–2163.

(12) Mong, G. M.S. Thesis, University of Wisconsin—Madison, 1979.

(13) Zimmerman, H. E.; Armesto, D.; Amezua, M. G.; Gannett, T. P.; Johnson, R. P. *J. Am. Chem. Soc.* **1979**, *101*, 6367–6383.

(14) (a) Footnote 12 in ref 14b suggests that structures should be firmly established by synthesis or degradation and notes the danger of NMR identification alone. This comment now needs modification to include the alternative of X-ray crystallography along with synthesis and degradation. (b) Zimmerman, H. E.; Tolbert, L. M. *J. Am. Chem. Soc.* **1975**, *97*, 5497–5507.

Our attention next focussed on the solution photochemistry of the tri-π-methane system **5**. This reactant had several intriguing aspects. One involved the regiochemistry and the question of which two vinyl groups would bond in the excited state. A particularly interesting question was whether the third vinyl group could participate in the mechanism (vide infra); mechanistic considerations suggested the possibility of obtaining a vinylcyclopentene rather than the usual di-π-methane product, a vinylcyclopropane. We have been attempting to effect such a rearrangement for many years.[12]

In solution, however, irradiation of trivinylmethane **5** afforded only cyclopropane products (eq 7). The structures were established by X-ray analysis. All three products arise from di-π-methane mechanisms. Further, sensitized photolyses were run for comparison purposes, and only divinylcyclopropane products were formed. The major product was cyclopropane **23**, and an additional divinylcyclopropane could be observed by NMR analysis but proved thermally unstable.

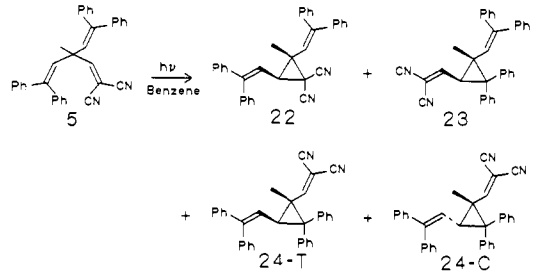

(7)

Exploratory Solid-State Photolysis Procedure. For exploratory irradiations the reactant was deposited on the inner walls of a cylindrical vessel by concentration of a reactant solution. Except for absence of solvent and cooling to 0 and −78 °C, the procedure for photolysis was the same as for solution irradiations. Conversions were carried out to the point where the product distribution began to be altered.

The Solid-State Photochemistry of the Di-π-methane Systems. With the solution photochemistry of di-π-methane systems **1–5** known, we turned to their solid-state counterparts. It was immediately apparent that the solid-state photochemistry of tetraphenyldicyano diene **1** differed dramatically from that of the solution counterpart. A single photoproduct **25** was formed, and the NMR spectrum revealed the presence of five vinyl absorptions and the loss of one phenyl group. X-ray crystallographic analysis led to the triphenyltricyclic structure for **25** shown in eq 8. This clearly was not a di-π-methane type product but rather the result of a $2_\pi + 2_\pi$ cycloaddition involving one phenyl group and the dicyanovinyl π-bond.

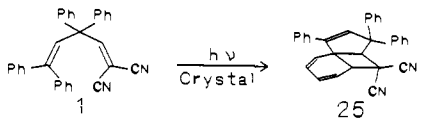

(8)

The solid-state irradiations of the structurally related diisopropyldicyano diene **2** and the dimethyldicyano diene **3** were investigated for comparison. Interestingly, while the diisopropyldicyano diene **2** followed the same reaction course as **1**, the dimethyldicyano diene **3** proved unreactive in the crystal. This chemistry is outlined in eq 9 and 10. The structure of the photoproduct **26** was established by X-ray crystallography.

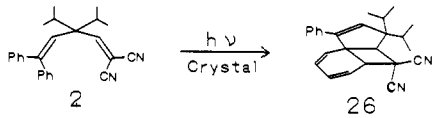

(9)

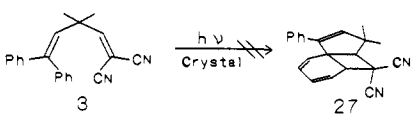

(10)

Table I. Crystal and Solution Photochemistry of 4,4-Diarylcyclohexenones

compd	solvent	product ratio *trans*-**30**	product ratio *cis*-**31**	product ratio 3,4-enone **32**
diphenylcyclohexenone **29a**	benzene	143	1	0.8
	crystal	1	0	0
dibiphenylcyclohexenone **29b**	benzene	10	1	0.8
	crystal	83	1	0
di-α-naphthylcyclohexenone **29c**	benzene	1	0	1.3
	crystal	1	0	0

Irradiation of the fourth di-π-methane reactant in the crystalline state provided another contrast with the solution photochemistry. Rather than the two di-π-methane photoproducts observed in solution, the crystalline photochemistry proceeded with complete, and reversed, regioselectivity as outlined in eq 11. In this case, the photoproduct structure was known from our solution-phase study described above.

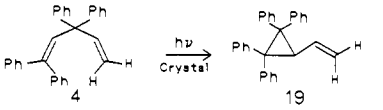

(11)

The last di-π-methane system might better be termed a "tri-π-methane" reactant, and this proved to provide the most striking result thus far. It was observed that the usual, solution di-π-methane photoproducts (note eq 7) were not encountered. Rather, a single photoproduct, mp 138 °C, was formed. This was initially identified by NMR spectral analysis which included the observation of two vinyl hydrogen peaks, one methine peak, and one allylic methyl peak with coupling consonant with vinylcyclopentene structure **28** (eq 12). This structural assignment was confirmed[14] by X-ray analysis. Clearly, this was the rearrangement we had been seeking for a decade.[12]

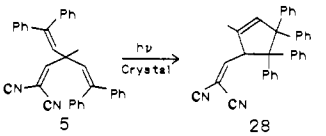

(12)

The Solution Photochemistry of 4,4-Diarylcyclohexenones. We next turned our attention to the solid-state photochemistry of the cyclohexenones. As a necessary prelude we need to consider the corresponding solution photochemistry. The solution photochemistry of the 4,4-diphenylcyclohexenone (**29a**),[16] 4,4-dibiphenylylcyclohexenone (**29b**),[17] and 4,4-di-α-naphthylcyclohexenone (**29c**)[18] has previously been studied in our laboratories (eq 13 and Table I).

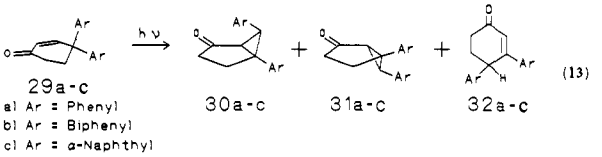

(13)

The Solid-State Photochemistry of 4,4-Diarylcyclohexenones. These compounds were unusual in the sense that their solid-state photochemistry was quite similar to that in solution. A major exception, however, was the near complete selectivity leading to the *trans*-5,6-diarylbicyclo[3.1.0]hexan-2-ones **30a–c**, and the complete absence of the 3,4-diarylcyclohex-2-en-1-ones **32a–c**,

(15) Pratt, A. C.; Alexander, D. W.; Rowley, D. H.; Tipping, A. E. *J. Chem. Soc., Chem. Commun.* **1978**, 101–102.[15b] (b) Interestingly, **16** is a minor photoproduct in the nonpolar solvent used by Pratt[15a] but a major one in polar solvents such as methanol. Thus it was not reported in ref 15a.

(16) (a) Zimmerman, H. E.; Wilson, J. W. *J. Am. Chem. Soc.* **1964**, *86*, 4036–4042. (b) Zimmerman, H. E.; Hancock, K. G. *J. Am. Chem. Soc.* **1968**, *90*, 3749–3760. (c) Zimmerman, H. E.; Elser, W. R. *J. Am. Chem. Soc.* **1969**, *91*, 887–896.

(17) Zimmerman, H. E.; Jian-Hua, X.; King, R. K.; Caufield, C. E. *J. Am. Chem. Soc.* **1985**, *107*, 7724–7732.

(18) Zimmerman, H. E.; Caufield, C. E.; King, R. K. *J. Am. Chem. Soc.* **1985**, *107*, 7732–7744.

characteristic of the solution photochemistry (eq 13 and Table I).

The Solution Photochemistry of the 5,5-Diphenylcyclohexenones. Previously we have reported[19] an unusual transformation of cyclohexenones having odd-electron stabilizing groups at C-5; in this reaction vinylcyclobutanones are formed. Thus 4-methyl-5,5-diphenylcyclohexenone (**33**) was found to afford 2-*trans*-propenyl-3,3-diphenylcyclobutanone (**34**) as in eq 14. Similarly,

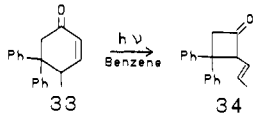

33 34 (14)

4,5,5-triphenylcyclohexenone (**35**) afforded the corresponding vinylcyclobutanone **36** as well as two phenyl migration products **37** and **38** in more typical cyclohexenone fashion (eq 15).

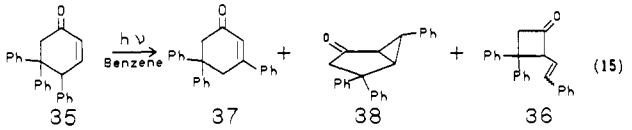

35 37 38 36 (15)

The Solid-State Photochemistry of the 5,5-Diphenylcyclohexenones. We first turned to the solid-state photolysis of 4,5,5-triphenylcyclohexenone **35**. Two photoproducts, **39** and **40**, were formed and proved not to correspond to any of the solution-phase products. X-ray analysis was employed to determine structures of these, which then permitted the photochemistry to be described as in eq 16. Clearly, the first photoproduct (i.e. **39**)

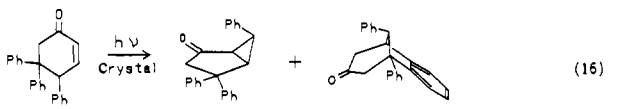

35 39 40 (16)

results from the same basic phenyl migration as the solution product **38** but with a reversed configuration at C-6 of the bicyclo[3.1.0]hexanone system. The second photoproduct **40** is seen to arise from bridging of the ortho position of a C-5 phenyl group with the β-carbon of the enone system.

In contrast, photolysis of crystalline 4-methyl-5,5-diphenylcyclohexenone (**33**) led to no reaction under extended irradiation conditions (eq 17).

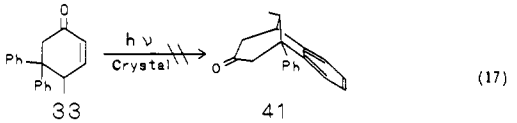

33 41 (17)

The Solution Photochemistry of an Unsaturated Alcohol. For this portion of our investigation we selected the photochemistry of 1,1,5,5-tetraphenyl-3,3-dimethyl-1-penten-5-ol (**42**). In our solution-phase studies we found an unusual long-range phenyl migration in which an aryl group migrates from the carbinol carbon to the excited styryl π-bond to afford ketone **43** (eq 18).[20]

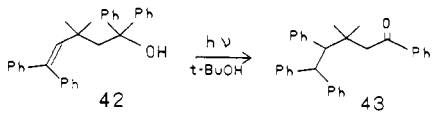

42 43 (18)

The photochemistry of crystalline **42** afforded two photoproducts **44** and **45**. The structures were established by independent synthesis (Scheme III). Interestingly, the oxidative-hydroboration of the known[20] unsaturated alcohol **42** led to two diols, one of which (i.e. **46**) was known.[21] Treatment of diol **46** with acid led to tetraphenyltetrahydropyran **44** which proved identical with one photoproduct. This compound had been described in earlier literature with limited characterization.[21] Similar acid treatment

(19) Zimmerman, H. E.; Solomon, R. D. *J. Am. Chem. Soc.* **1986**, *108*, 6276–6289.
(20) Zimmerman, H. E.; Nuss, J. M. *J. Org. Chem.* **1986**, *51*, 4604–4617.
(21) Wittig, G.; Overman, B. *Chem. Ber.* **1934**, *67B*, 2053.

Table II. Solid-State Quantum Yields and Corresponding Solution Values

reactant	solvent	quantum yield	photoproduct
tetraphenylpentadiene **4**	acetonitrile	0.060	cyclopropane **19**
		0.073	cyclopropane **20**
		0.133	total
	solid	0.015	cyclopropane **19**
triene **5**	benzene	0.043	cyclopropane **22**
		0.057	cyclopropane **23**
		0.050	cyclopropane **24T**
		0.027	cyclopropane **24C**
		0.177	total
	solid	0.0008	cyclopentene **28**
biphenylcyclohexenone **29b**	*tert*-butyl alcohol[b]	0.26	trans-bicyclic **30b**
		0.024	cis-bicyclic **31b**
		0.020	3,4-enone **32b**
		0.304	total
	solid	0.010	trans-bicyclic **30b**
		0.00012	cis-bicyclic **31b**
1-naphthylcyclohexenone **29c**	benzene[c]	0.43	trans-bicyclic **30c**
		0.57	3,4-enone **32c**
		1.00	total
	solid	0.0061	trans-bicyclic **30c**
triphenylcyclohexenone **35**	*tert*-butyl alcohol[d]	0.087	3,5,5-enone **37**
		0.031	exo-bicyclic **38**
		0.037	cyclobutanones **36**
		0.155	total
	solid	0.00003	endo-bicyclic **39**
pentenol **42**	*tert*-butyl alcohol[e]	0.0026	pentanone **43**
	solid	0.0055	tetrahydropyran **44**
		0.0073	tetrahydrofuran **45**
		0.0128	total

[a] Estimated error ±10%. [b] Reference 17. [c] Reference 18. [d] Reference 19. [e] Reference 20.

Scheme III. Synthesis of Photoproducts **44** and **45**

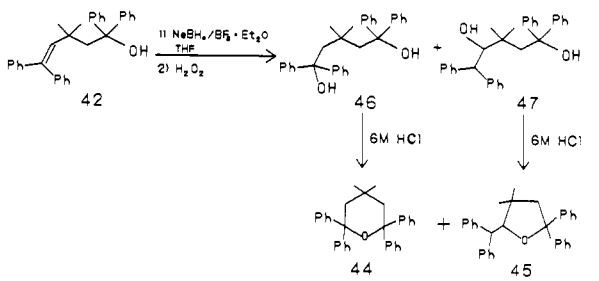

42 46 47 44 45

of diol **47** afforded tetrahydrofuran **45**, the second solid-state photoproduct. Hence the irradiation of the crystalline material may be depicted as in eq 19.

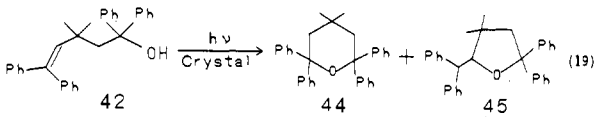

42 44 45 (19)

Solution Quantum Yields. Many of the solution quantum yields needed for this study were reported earlier. However, the solution quantum yields of tetraphenylpentadiene **4** and tri-π-methane reactant **5** were obtained by methods described in our earlier papers and in the Experimental Section. These results are included in Table II.

Solid-State Quantum Yields. The solid-state quantum yields were obtained with use of the microbench and monochromator combination[22] used in our work for solution quantum yields.

(22) Hatchard, C. G.; Parker, C. A. *Proc. R. Soc. London, Ser. A* **1956**, *235*, 518–521.

Table III. Correlation of Calculated Reactivity Parameters[a] with Observation

		to photoproduct			to diradical species				
reactant	photoproduct	ΔM, Å/atom	ΔV, %	ΔS, %	diradical	ΔM, Å/atom	ΔV, %	ΔS, %	state[b]
dicyano triene **5**	cyclopropane **22**	1.70	38	16	**55**	0.78	15	5	soln
	cyclopropane **23**	2.20	41	11	**56T**	1.87	26	10	soln
	cyclopropane **24T**	1.39	32	13	**57**	0.53	15	2	soln
	cyclopropane **24C**	1.71	40	13	**57**	0.53	15	2	soln
	cyclopentene **27**	1.37	35	6	**56C**	0.24	6	1	solid
diphenyl enone **29a**	trans-bicyclic **30a**	1.09	28	14	**60a**	0.92	21	15	both
	cis-bicyclic **31a**	1.21	29	17	**61a**	0.92	29	22	soln
	3,4-enone **32a**	1.76	45	25	**61a**	0.92	29	22	soln
dibiphenyl enone **29b**	trans-bicyclic **30b**	1.55	34	20	**60b**	1.37	25	4	both
	cis-bicyclic **31b**	3.20	42	29	**61b**	4.18	32	25	soln
	3,4-enone **33b**	3.37	46	28	**61b**	4.18	32	25	soln
naphthyl enone **29c**	trans-bicyclic **30c**	1.50	33	18	**60c**	0.46	11	2	both
	3,4-enone **33c**	1.84	35	21	**61c**	1.09	21	6	soln
methyl enone **33**	cyclobutanone **34**	0.90	19	12	**62**	0.35	8	6	soln
	benzobicyclic **41**	0.58	11	6	**65**	0.65	10	4	none
triphenyl enone **35**	endo-bicyclic **39**	0.72	24	1	**63**	1.15	25	4	solid
	benzobicyclic **40**	0.64	21	3	**65**	0.65	18	1	solid
	exo-bicyclic **38**	1.49	32	12	**64**	1.18	27	9	soln
	triphenyl enone **37**	1.27	29	17	**64**	1.18	27	9	soln
	cyclobutanone **36**	1.24	38	11	**62**	0.55	16	4	soln
pentadiene **1**	cyclopropane **8**	2.00	52	28	**69a**	0.79	20	6	soln
	cyclopropane **9**	2.06	28	17	**20a**	0.87	20	5	soln
	cyclopropane **10**	1.88	39	16	**67a**	0.63	17	6	soln
	tricyclo triene **25**	1.01	20	7	*c*				solid
pentadiene **2**	cyclopropane **11**	1.54	36	17	**69b**	0.86	18	5	soln
	1,3-diene **12**	1.09	30	8	*d*	0.60	19	3	soln
	1,3-diene **13**	1.09	26	8	*d*	0.60	19	3	soln
	1,4-diene **14**	0.45	20	3	*d*	0.60	19	3	soln
	tricyclo triene **26**	1.04	22	6	*c*				solid
pentadiene **3**	cyclopropane **15**	0.96	19	10	**68c**	0.55	14	4	soln
	housane **16**	1.59	12	9	*c*				soln
	tricyclo triene **27**	1.39	15	8	*c*				solid
pentadiene **4**	cyclopropane **19**	0.98	28	7	**68d**	0.81	25	2	both
	cyclopropane **20**	1.19	34	12	**67d**	0.86	27	7	soln
pentenol **42**	pentanone **43**	1.08	26	9	**71**	1.00	18	5	soln
	ether **44**	0.73	21	4	**72**	0.20	8	2	solid
	ether **45**	0.73	21	3	**73**	0.20	8	1	solid

[a] See text for definitions. [b] State of reactant photolyzed which results in the formation of the photoproduct. [c] Not applicable. [d] The radical pair was used as the species past the branch point; however, the mechanism for these rearrangements may not proceed via the radical pair.

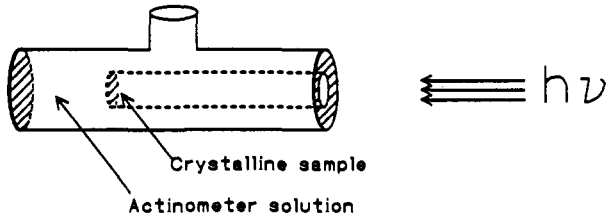

Figure 1. Solid-state quantum yield cell.

However, a special quartz cell (Figure 1) was designed for solid-state runs. The crystalline material was packed between two quartz plates and placed in the inner cavity in the quartz cell as shown. Light not captured by the sample is absorbed by the surrounding potassium ferrioxalate solution, and the depth of the cavity is sufficient that less than 4% of the scattered light could emerge from the cavity entrance (cf. Experimental Section). Finally, the quantum yields obtained are summarized in Table II.

Reactant X-ray Structures. For understanding the course of the solid-state photochemical transformations X-ray structures of the reactants were obtained. A further point to be noted is that the crystals used for the X-ray structures were demonstrated to be the same as those subjected to photolysis. This was done by comparing polycrystalline X-ray diffraction patterns (powder patterns) of samples used for photolysis with powder patterns calculated from the single-crystal diffraction data.

Generation of Branch Point and Photoproduct Structure Conformations. A method for predicting the outcome of solid-state photochemical rearrangements based on comparing the reactant X-ray structure with the structures of potential photoproducts was sought. It seemed that in some rearrangements, structures of photoproducts are irrelevant since the reaction course is determined at some point much earlier along the reaction coordinate; we term this the "branch point". Thus photoproduct structures and structures of diradical species just past the branch point were required.

Although X-ray structures were available for many of the photoproducts, the conformation of the molecule in an independently prepared crystal differs from the conformation of the molecule generated by reaction in the reactant crystal. What promised more utility were structures of photoproducts and diradical species generated by taking that conformation which had the maximum congruence with the corresponding reactant. In each case molecular mechanics was used to generate a structure of the desired product or species. This structure was then subjected to superimposition by MACROMODEL[23] with variation of torsional angles and maintenance of bond lengths and valence angles. The

(23) Still, W. C.; Mohamadi, F.; Richards, N. G. J.; Guida, W. C.; Caufield, C.; Liskamp, R.; Hendrickson, T.; Chang, G., MacroModel V2.0, Columbia University, New York, NY 10027.

Scheme IV. Solution Photochemistry of a Tri-π-methane System

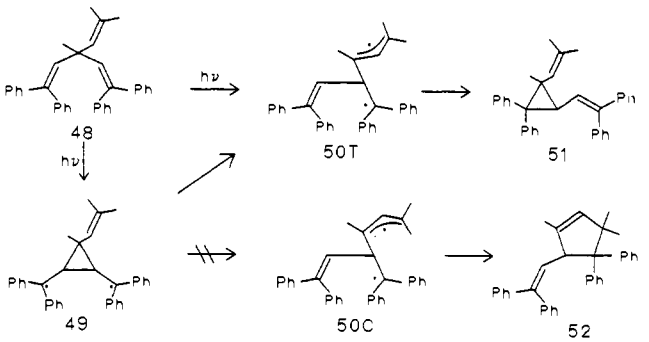

net effect was maximization of the congruence of reactant and the potential product or branch point species.

Computational Methodology. Motion. One factor that has been considered in the literature has been "least motion".[9] We were interested in assessing the utility of a quantitative approach in which the sum of the atomic displacements in proceeding from reactant to branch-point or photoproduct structure was used. Since all of the atomic displacements are positive, we elected to take the simple summation of all non-hydrogen atom displacements in proceeding from the X-ray structure of reactant to the superimposed (vide supra) product or branch point species. These reactivity parameters (the ΔM's) are included in Table III.

Computational Methodology. Volume Requirement. As in the least motion treatment above, the corresponding volume change (ΔV) on reaction was computed in proceeding from the X-ray structure of reactant to the superimposed product or branch point species. In order to obtain the volume of each species a modification of the volume routine used in the TRIBBLE package[24] was employed. The volume change (ΔV) is calculated as the volume of the superimposed species not common with the reactant. The resulting ΔV's are given in Table III.

Computational Methodology. Lattice Interference. The third approach to quantitative predictions of reactivity was based on the ability of the superimposed product or diradical species to fit into the reactant crystal lattice. This was done by computationally superimposing one product or branch point molecule on a reactant molecule in the crystal lattice and then extracting the reactant molecule. The net result is that the inserted molecule is placed in the lattice so that it conforms optimally to the orientation of the reactant molecule it replaces. Then, the overlap (ΔS) of the inserted species with the surrounding reactant molecules of the crystal lattice was determined

$$\Delta S = (V_h + V_r - V_m)/(V_h + V_r) \qquad (20)$$

where V_h is the volume of crystal lattice segment with one reactant molecule removed, V_r is the volume of a product or branch point species, and V_m is the volume of a crystal lattice segment containing the product or branch point species. To the extent that there is overlap, the volume of the lattice containing the photoproduct or diradical species will be less than the sum of the two individual volumes. This difference is the overlap with neighboring reactant molecules. A lattice segment large enough to contain the entire superimposed species was used. The overlaps (ΔS) found are included in Table III.

Discussion

The Tri-π-methane Rearrangement. As noted earlier, for quite some years we have been attempting to obtain what may be termed a "tri-π-methane rearrangement" by having vinyl substitution on the central, methane carbon of a di-π-methane system. Thus we have studied[12] the solution photochemistry of trivinylmethane **48**. The hope was that after opening of cyclopropyl dicarbinyl diradical **49**, the 1,3-diradical species **50** would close to form a cyclopentene (i.e. **52**) rather than the usual cyclopropane (i.e. **51**) as depicted

(24) Pensak, D. *Ind. Res. Dev.* **1983**, *25*, 74–78.

Scheme V. Solution Photochemistry of Tri-π-methane Reactant **5**

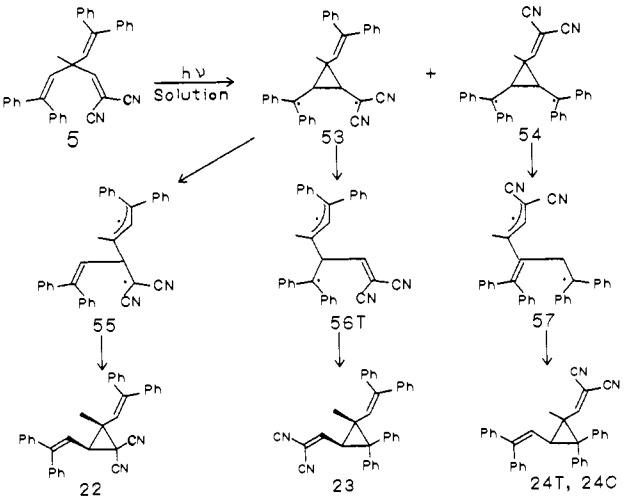

Scheme VI. Solid-State Photochemistry of Tri-π-methane Reactant **5**

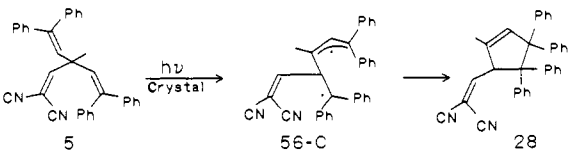

in Scheme IV. However, all such attempts were unsuccessful and only the usual di-π-methane products were observed. The lack of success was ascribed[12] to the allylic moiety being s-trans and thus incapable of closing to a *cis*-cyclopentene. It was in the hope that incorporation in a crystal lattice would enforce an s-cis conformation that we pursued this reaction further. As noted above the photochemistry of tri-π-methane **5** in crystalline medium did, indeed, lead completely to the desired cyclopentene in complete contrast to the ordinary solution di-π-methane rearrangement. The solution photochemistry is outlined in Scheme V while the crystal photochemistry is given in Scheme VI.

With respect to the solution photochemistry of tri-π-methane **5** there are several points needing discussion. We note that there are two competitive initial bridging steps—bridging diphenylvinyl to dicyanovinyl and diphenylvinyl to diphenylvinyl (note Scheme V). The product distribution in low-conversion irradiations suggests that these are approximately equally competitive (1:1.1). This is consistent with the results found[13] for the two isomeric di-π-methane systems, **1** and **58**, where in each case one of the two types of bridging is enforced (diphenylvinyl–dicyanovinyl bridging in **1** and diphenylvinyl–diphenylvinyl in **58**) and where the quantum yields for the two reactants are in a ratio of 1:1.2.

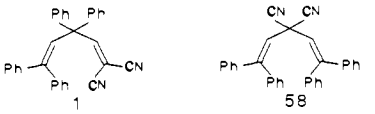

Turning now to the photochemistry of crystalline tri-π-methane **5** we recognize the cisoid conformation of diradical **56** necessary for cyclopentene formation may be envisaged as enforced by the confines of the surrounding crystal lattice (note Scheme VI and Figure 2). In addition, formation of the cisoid 1,3-diradical **56-C** has smaller reactivity parameters than the mechanism via the transoid 1,3-diradical **56-T** which leads to cyclopropane product. That is, less molecular motion, less molecular volume increase, and less overlap with the surrounding crystal lattice occurs on formation of the transoid diradical. Interestingly, the same criteria hold if we consider the molecular change leading all the way to final cyclopentene product **28**. The parameters are included below in our generalization of solid-state reactivity.

4,4-Diarylcyclohexenone Photochemistry. The crystalline photochemical behavior of these compounds proved a contrast to

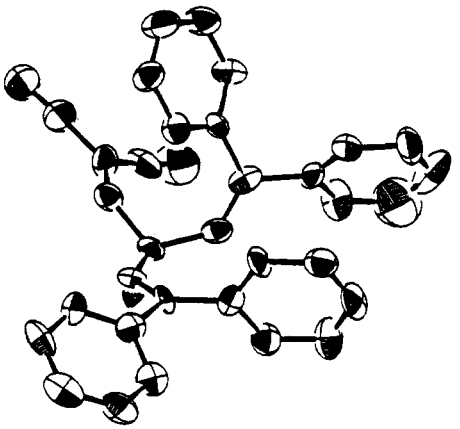

Figure 2. ORTEP drawing of dicyano triene 5.

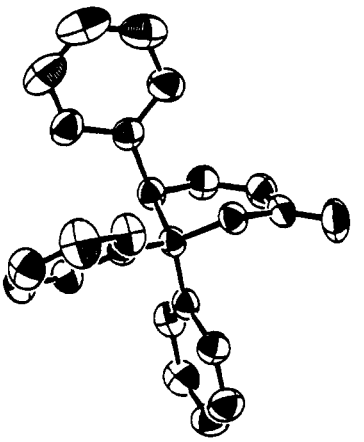

Figure 3. ORTEP drawing of triphenylcyclohexenone 35.

Scheme VII. Solid-State and Solution Mechanisms of Cyclohexenone Rearrangements

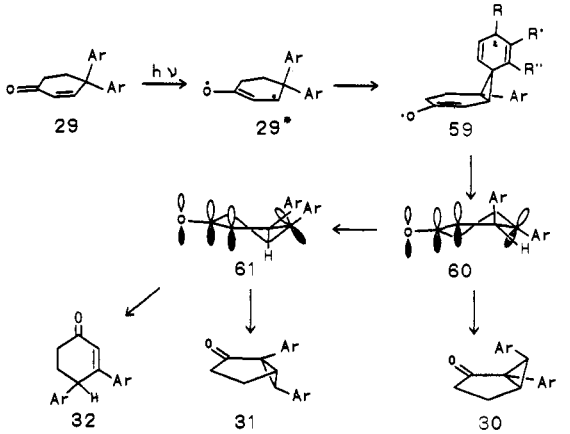

Scheme VIII. Solution and Crystal Mechanisms of Triphenylcyclohexenone 35

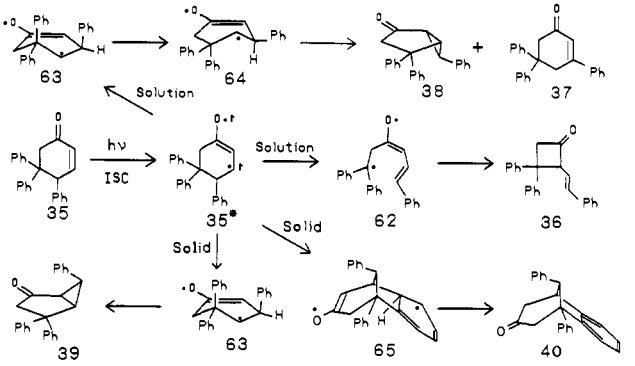

the tri-π-methane systems just discussed. Thus completely different photochemistry was not observed in the solid. The common feature of the crystalline photochemistry of these enones was the complete absence of the 3,4-diarylcyclohexenone products **32a–c** and the near complete absence of the *cis*-5,6-diarylbicyclo[3.1.0] isomers **31a–c**. Table I gives a comparison of the product distributions in the crystal compared to solution.

Scheme VII shows the general mechanism for these reactions. It is seen that the pseudoaxially oriented aryl group migrates from C-4 to C-3 of the excited enone as in diradical **60**. In this conformer it is seen that there are two lobes of the C-2 and C-4 p-orbitals that are aimed inwards and towards one another and are capable of forming a three-ring; these are the lobes anti to the migrated aryl group. In this three-ring closure, the migrated aryl group becomes endo and trans to the nonmigrating aryl moiety at C-4. The net stereochemistry is the ubiquitous inversion of configuration at C-4 seen in solution.

The formation of 3,4-diarylcyclohexenones is seen to result from a conformational flip to afford diradical **61** which has the C-3 hydrogen now pseudoaxial and then capable of migration to C-4 to afford the 3,4-diarylcyclohexenone **32**. Additionally, in diradical conformer **61** the p-orbital lobes aimed at one another are those that are syn to the migrated aryl group; bonding between these is seen (note Scheme VI again) to lead to formation of the exo (i.e. cis) stereoisomer of the bicyclo[3.1.0]hexanone **31**.

The Case of the Solid-State Photochemistry of 4,5,5-Triphenylcyclohexenone (35). Just as the solution photochemistry of cyclohexenones doubly substituted at C-5 with phenyl groups is unusual, the solid-state photochemistry proved so. First we note that the photochemistry of crystalline **35** gave none of the solution-phase photoproducts. The solution photochemistry for this enone was unique in not affording the *endo*-5,6-diphenyl bicyclic stereoisomer **39** (Scheme VIII). Instead, the usually minor *exo*-5,6-diphenyl bicyclic isomer **38** and the aryl-migrated cyclohexenone **37** were major products. In the solution photochemistry one expects initial formation of the pseudoaxial conformer of the phenyl-migrated diradical **63**; however, steric repulsion between two axially oriented phenyl groups directs the mechanism to diradical conformer **64**. Using the reasoning in the preceding section, we note that this conformer has appropriate stereochemistry for formation of the *exo*-5,6-diphenylbicyclic product **38** and the 5,5,3-triphenylcyclohexenone product **37** (Scheme VIII).

Thus we see that the solution photochemistry requires a dramatic geometric conformational change in which the compact diradical **63** with two axial phenyl groups led to extended conformer **64** with two equatorial phenyls. This suggested that the photochemistry of the crystal might inhibit these geometric changes, which was indeed the case. Hence, we can interpret the formation of the endo stereoisomer as resulting from the crystal constraining diradical **63** to a compact geometry as it reacts and inhibiting the conformational ring flip. In addition, the reactivity indices were much lower for the formation of the endo stereoisomer. A final point is that the X-ray of triphenylcyclohexenone **35** reveals the C-4 phenyl group to be axial prior to migration, and thus the molecule starts in a compact conformation (Figure 3).

The second solid-state photoproduct is benzobicyclic ketone **40**. Inspection of the X-ray structure of reactant **35** shows the proximity of the β-enone carbon and the ortho carbon of the axial C-5 phenyl group. Since after bridging a hydrogen atom needs to be transferred from this ortho carbon to the α-carbon of the six-ring, a small twist of the phenyl group is required to permit the more remote p-orbital lobe of the ortho carbon to bond.

The ΔM parameter, along with ΔV and ΔS, is given in Table III for both the solid and solution reactions, and these values are seen to be smaller in each case for the solid photochemistry.

Comparison of the 4-Methyl-5,5-diphenylcyclohexenone. Interestingly, the closely related 4-methyl-5,5-diphenylcyclohexenone proved unreactive in the photochemistry of the crystal. Of course,

Table IV. Vinyl–Phenyl Orientation and Proximity[a,b] in the Di-π-methane Systems

reactant	*A*	*B*	av	d_1	d_2	d_{av}	twist angle θ, deg
diphenyl diene **1**	2.90	3.26	3.08	0.33	0.02	0.17	36.1
diisopropyl diene **2**	2.89	3.54	3.21	0.45	0.39	0.45	13.9
dimethyl diene **3**	2.95	3.64	3.30	0.86	0.73	0.79	64.3

[a] See Figure 5. [b] d_1 and d_2 are the displacements between the bonding centers from a projection of the vinyl group into the plane of the phenyl group.

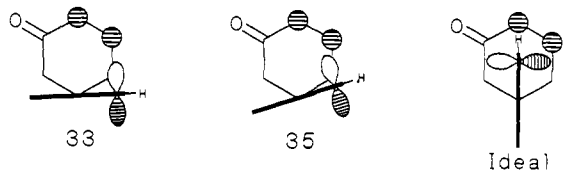

Figure 4. Conformational differences in the methyldiphenyl and triphenyl enones.

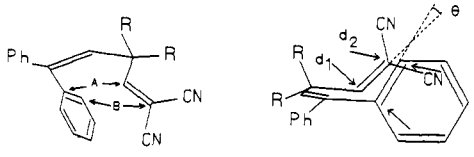

Figure 5. The geometry of the di-π-methane systems.

in the absence of a C-4 phenyl group one is concerned with just the ortho to β-enone bonding reaction. We note that two of the three reactivity parameters, ΔM and ΔV, are low and favorable relative to the 4,5,5-triphenylcyclohexenone **35**. ΔS, while twice the value for the triphenyl analogue, still is small (Table III). This illustrates a limitation of the present reactivity parameters (vide infra) which are primarily useful in the prediction of how a reaction will proceed rather than whether or not the reaction will occur. Where crystalline compounds are unreactive, there are generally specific reasons extraneous to the factors governing the reactivity parameters.

In the present instance, the reaction might be considered to be controlled more by proximity than confinement. The ortho to β-carbon distance in the reactive triphenyl enone is 3.12 Å while in the unreactive methyl case it is 3.34 Å. This is not reflected in ΔM, since ΔM for the triphenyl example results from a large number of atoms at the different phenyl groups which are displaced and contribute; thus there is lack of parallelism between motion and proximity.

A more likely factor can be seen in Figure 4. For successful reaction as in the triphenyl case (**35**), not only must the *o*-phenyl carbon bond to the β-enone carbon but additionally the hydrogen at the ortho carbon must become syn to the α-enoloxy carbon of the resulting diradical for the subsequent hydrogen transfer to be possible. This requires bonding of the back lobe of the ortho p-orbital as in the ideal conformation in Figure 4 (note also structure **65** in Scheme VIII). If instead the front lobe of that p-orbital bonds, then the hydrogen becomes disposed anti as in structure **33** in Figure 4. The X-ray structures for the triphenyl enone **35** and the methyldiphenyl enone **33** do differ by 14.4° in the rotation of the axial C-5 phenyl group in the direction shown in Figure 4. This predicts that the methyldiphenyl enone **33** is more likely to reversibly afford a nonreactive diradical.

The Dicyano-Substituted Di-π-methane Systems. The first two of the three di-π-methane systems having terminal dicyano substitution, compounds **1**, **2**, and **3**, underwent a $2_\pi + 2_\pi$ cycloaddition of the dicyanovinyl group with the ipso-C-2 bond of the *cis*-phenyl group while the third component (i.e. **3**) is unreactive. Reference to Figure 5 and Table IV reveals that the positioning is excellent for the 2 + 2 electrocyclic addition in the cases of reactants **1** and **2** but less favorable for **3**. Schmidt[25] has suggested that 2 + 2 cycloadditions will occur when the distance between π-bonds is 4.2 Å or less and with optimum orientation. In the present instance, although the intergroup distances for all three compounds are within this distance, **3** has the largest separation. Additionally, the orientation for **3** is less than optimal with the inter-π-bond twist angle (θ) being 64° and larger than for **1** and **2**. In addition there is an appreciable lateral displacement in the case of reactant **3**. Table IV lists these differences.

Scheme IX. The Mechanism of the Di-π-methane Rearrangement

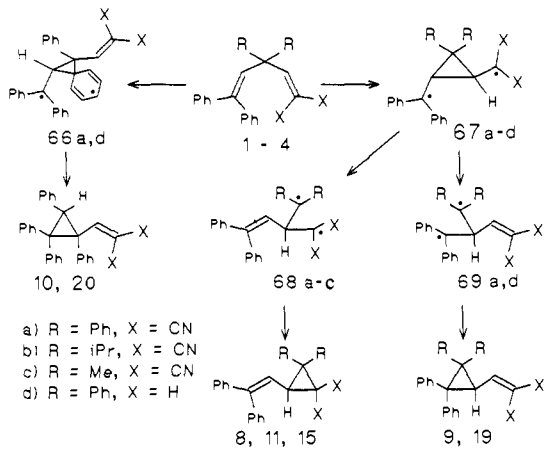

In terms of the reactivity parameters of the present study, primarily ΔM differs among the three reactants, being larger for the nonreactive **3** (note Table III). While more motion is required for **3** to react, the volume and overlap parameters differ little among **1**, **2**, and **3**.

These examples provide an illustration of the limitation of the present reactivity parameters. In these 2 + 2 cycloadditions, there is very little molecular motion, and our reactivity parameters tend to be small. However, the three reactivity parameters—ΔM, ΔV, and ΔS—are permissive in the sense of indicating only when too much motion is involved or insufficient space is available for reaction. When the reactivity parameters are small, it is still possible that factors such as an inherently high activation barrier may inhibit reactivity.

The Solid-State Photochemistry of 1,1,5,5-Tetraphenyl-1,4-pentadiene (4). The crystal photochemistry of this compound led to one product, this resulting from a regioselective di-π-methane rearrangement (Scheme IX) to afford tetraphenylvinylcyclopropane (**19**) (note eq 11). The photochemistry in the crystal thus

(25) (a) In the case of least motion, very recently the idea of using the sum of the root-mean-square displacements in proceeding from reactant to final product has been advanced[25b] to rationalize relative reactivity of two compounds in the crystalline state. The product structures used have been derived from X-ray determination. As Scheffer has noted,[25d] this assumes that during photolysis in the crystal the product will adopt the geometry of the recrystallized material. (b) Thomas, N. W., unpublished work, cited in the chapter by Theocharis, C. R.; Jones, W. in ref 6c.[25c] (c) A single example was given in which the root-mean-square sum differed by 4% between two different reactants. (d) More recently, this index has been used in one case by: Scheffer, J. R.; Trotter, J.; Garia-Baribay, M.; Wireko, F. *Mol. Cryst. Liq. Cryst. Inc. Nonlin. Opt.* **1988**, *156*, 63–84. (e) The reactant and product geometry was taken from X-ray data in ref 25d while ref 25b did not clarify this point.

(26) (a) It needs to be noted that very recently two efforts have been reported to consider the energetic consequences of deforming reactants toward product. One example is the computation of intermolecular methyl–methyl repulsion between two β-methyl groups of adjacent enones as a consequence of intramolecular hydrogen transfer to the β-position of one of the molecules.[26b] In the same publication, discussions of intermolecular repulsions are considered. (b) Ariel, S.; Askari, S.; Evans, S. V.; Hwang, C.; Jay, J.; Scheffer, J. R.; Trotter, J.; Walsh, L.; Wong, Y-F. *Tetrahedron* **1987**, *43*, 1253–1272. (c) A further study[26d] has been reported in which the cyclodimerization of enones and related compounds is considered relative to the packing potential energy change on bringing polarized π-bonds together positioned for π–π overlap. Of four unreactive reactants of the series, two are predicted to react, hence it may be that one needs to consider conformational change within the molecule. (d) Murthy, G. S.; Arjunan, P.; Venkatesan, K.; Ramamurthy, V. *Tetrahedron* **1987**, *43*, 1225–1240.

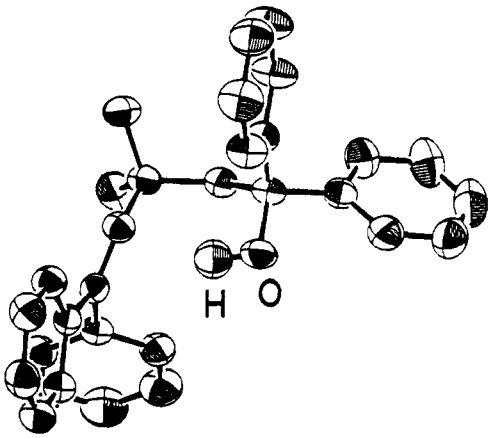

Figure 6. ORTEP drawing of tetraphenylpentenol **42**.

Scheme X. Mechanisms of Rearrangement of Tetraphenylpentenol **42**

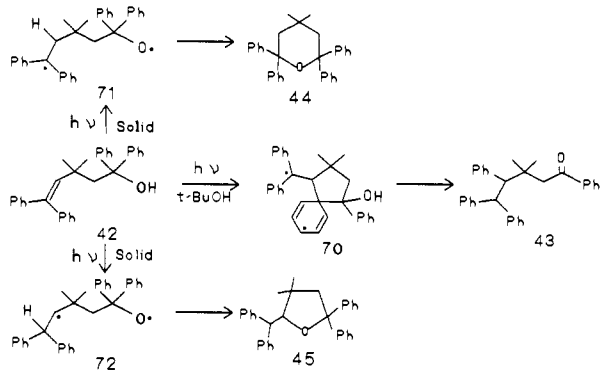

proves completely regioselective compared with the solution photochemistry (note eq 6). The preferred regioselectivity is seen to proceed via the reaction having the lowest reactivity parameters in Table III. An alternative rationale is that in the crystal it is the triplet that is rearranging, and this cannot rigorously be excluded.

The Solid-State Photochemistry of Tetraphenylpentenol 42. One of the unusual types of solution photochemistry we have encountered recently is the long-range phenyl migration encountered in the photochemistry of 1,1,5,5-tetraphenyl-3,3-dimethylpent-1-en-4-ol (**42**). As noted in the Results Section, the crystal photochemistry led to entirely different products, namely to tetrahydropyran **44** and tetrahydrofuran **45**.

Inspection of Table III shows that the three reactivity parameters are markedly lower for the reactions observed in the solid than for those observed in the solution processes. The mechanisms for both solution and crystal reactions are given in Scheme X. The observed solid-state photochemistry is conceptually reasonable since the phenyl migration reaction involves movement of an entire phenyl group while the hydroxyl addition requires less total motion. The X-ray structure of this reactant (note Figure 6 for an ORTEP drawing) reveals the reactant to have a coiled conformation, quite inappropriate for 1,4-phenyl migration but suitable for the observed hydroxyl addition to the diphenylvinyl bond. The reactivity parameters are seen to be similar for the two observed crystal photochemical reactions, that is, leading to the five- and six-membered rings. However, as noted below, our reactivity indices merely provide information about one source of control of reactivity. Superimposed on the effect of the crystal lattice are the usual energetic factors of electronic and steric origin.

It also needs to be noted that one might consider proximity of the reacting groups as rationalizing the observed reactivity. The hydroxyl–diphenylvinyl distances are 3.44 and 2.92 Å (for 6- and 5-membered-ring formation, respectively) while the phenyl–diphenylvinyl distance (to the ω-styryl carbon) is 3.59 Å. Thus one might suggest that hydroxyl addition is favored by proximity. In any case, proximity does not rationalize the near equal distribution of the 6- and 5-membered-ring photoproducts, since the distances for the two processes are quite different and the reactivity parameters seem to afford a better prediction.

Table V. Summary of X-ray Crystal Preparation

compd	crystallization method	crystallization solvent	crystal dimensions (mm)
pentadiene **1**	vapor diffusion	hexane/ethyl acetate	1.0 × 0.9 × 0.8
pentadiene **2**	vapor diffusion	hexane/ethyl acetate	1.0 × 0.4 × 0.1
pentadiene **3**	slow cooling	hexane	0.5 × 0.2 × 0.1
pentadiene **4**	slow cooling	methanol	1.0 × 0.9 × 0.6
triene **5**	slow cooling	hexane	0.5 × 0.4 × 0.2
cyclohexenone **29a**	slow cooling	hexane	1.0 × 0.1 × 0.1
cyclohexenone **29b**	slow evaporation	hexane	0.1 × 0.2 × 0.2
cyclohexenone **29c**	vapor diffusion	hexane/ toluene	1.1 × 0.9 × 0.5
cyclohexenone **33**	slow cooling	hexane	0.7 × 0.6 × 0.5
cyclohexenone **35**	slow cooling	hexane	0.9 × 0.8 × 0.6
cyclopropane **22**	slow cooling	2-propanol	0.3 × 0.2 × 0.2
cyclopropane **23**	slow cooling	2-propanol	0.5 × 0.1 × 0.05
cyclopropane **24T**	slow cooling	2-propanol	0.5 × 0.1 × 0.1
cyclopropane **24C**	slow cooling	2-propanol	0.1 × 0.05 × 0.05
pentenol **42**	slow cooling	2-propanol	0.9 × 0.7 × 0.5
tricyclic **25**	vapor diffusion	hexane/ethyl acetate	0.2 × 0.1 × 0.05
tricyclic **26**	slow cooling	2-propanol	0.5 × 0.4 × 0.4
bicyclic **39**	slow cooling	2-propanol	0.8 × 0.5 × 0.6
bicyclic **40**	slow cooling	2-propanol	1.0 × 0.6 × 0.1
housane **16**	slow cooling	2-propanol	0.4 × 0.3 × 0.2
cyclopropane **17**	slow cooling	2-propanol	1.0 × 0.8 × 0.5

Discussion of the Solid-State Reaction Efficiencies. A first observation is that the crystal photochemical quantum yields, with one exception, are quite low compared with the solution efficiencies. Realizing that quantum yields are given by the excited-state rate constant divided by the total rate of radiationless decay, we recognize that these generally low efficiencies cannot be understood on the basis of changes in excited-state decay rates (i.e. the denominator of the quotient alone). Since in general excited-state lifetimes, both singlet and triplet, are longer and rates of radiationless decay are smaller in solid phases—the quantum yields could only be enhanced by a lifetime effect. Thus the observed differences must arise from the rates of excited-state reaction (i.e. the numerator).

One interpretation of inhibited excited-state rates of reaction is that in those cases where crystal photochemistry differs from solution, the reaction which is energetically preferred in solution is inhibited by crystal lattice constraints with the result that one observes only the reaction corresponding to a process not having the lowest activation energy in solution. This result arises from the imposition of energetic contributions from crystal effects.

In addition, general restriction to motion will tend to lower reaction efficiencies, and some quantum yields for the same reaction are seen to be low.

In any case, this means that using crystal photochemistry, one often can inhibit the kinetically favored solution reactions and observe the "second best or third best" reaction.

However, one cannot assume that invariably quantum yields in the crystal will be lower than those in solution. For example, in bimolecular $2_\pi + 2_\pi$ cycloadditions, crystal lattices with the two molecules in proper proximity and orientation could in principle give rise to higher efficiencies in the crystal. Similarly, we note that in tetraphenylpentenol **42** the crystal efficiency for hydroxyl addition to the styryl π-bond with cyclization is considerably higher than the rather low quantum yield for the reaction observed in solution, namely 1,4-phenyl migration. The quantum yield for the cyclization reaction in solution must be still lower, since it is unobserved.

It appears that high crystal quantum yields compared to solution may occur in those cases where a specific conformation is required for the reaction, and this conformation is available in the crystal but in solution only via an unfavorable preequilibrium step.

The Validity of the Theoretical Approaches. In our studies we have used reactant geometry derived from X-ray along with both product and partially reacted geometries along the reaction co-

ordinate. Furthermore, for reactions proceeding with complex rearrangements, it seems likely that reactivity is determined much before product along the reaction coordinate. Thus, the concept of "branch point" geometries provides a parallel to transition-state control in solution photochemistry.

By taking the product and the branch point species and requiring that their geometries be superimposed, to the extent possible, on that of reactant, we provide species in the conformation most likely to be engendered during the reaction. The geometries of the product in an independently derived crystal seem subject to the risk of being unrelated to the geometry resulting during irradiation. Our use of the sum of the atomic displacements rather than the root-mean-square sum seems to provide an adequate measure of geometric change. Thus Table III does give a good correlation of least motion prediction with observed crystal reactivity.

The idea of using incremental volume to assess reactivity seems promising since development of new volume seems likely to be inhibited by the surrounding crystal lattice. Again, the correlation with observation is good (Table III).

A more direct way of getting at interference with the surrounding crystal lattice was provided by the overlap measurements detailed in the Results and Experimental Sections. Since the method used product or partially reacted molecules which were maximally oriented to conform with reactant, this method seemed likely to generate species as they would arise in the crystal rather than as they would exist in an independently crystallized product. Inspection of Table III reveals an excellent correlation of minimal overlap with preferred reactivity. Interestingly, in many of the cases use of the reactivity increments from reactant to final product correlates as well as the increments from reactant to the partially reacted species.

Limitations of the Reactivity Parameters. The comment is needed that the reactivity parameters alone are not capable of predicting when a reaction will occur or not. For example, two unreactive systems studied (**3** and **33**) have low reactivity parameters. Thus, one needs to consider, inter alia, electronic and other effects controlling solution reactivity; clearly, the reactivity parameters just assess additional constraints on reactivity which arise from incorporation in a crystal lattice.

Another aspect is the relationship between the reactivity parameters used in this study and control by proximity (e.g. of molecules or groups). It is seen that when two groups are in proximity and potentially might undergo a transformation not involving much molecular motion, the reactivity parameters are also likely to be small and predict reaction. However, for more complex reactions where considerable molecular reorganization occurs, it seems likely that proximity of initially bonding groups will be insufficient a criterion to predict reactivity. Here the reactivity parameters provide a necessary but insufficient requirement for reaction. The utility of these parameters needs further exploration to assess their general applicability.

Conclusion. General Observations Regarding Crystal versus Solution Photochemistry. We note that the crystal phase photochemistry promises to provide reactivity not accessible in solution. Additionally, crystal photochemistry seems to be considerably more selective in those cases where solution photochemistry gives rise to multiple product formation. However, the study of crystal photochemistry of complex systems lies mainly in the future, since only a relatively small number of molecular systems has been investigated.

Experimental Section[27]

1,1,3,3-Tetraphenyl-1,4-pentadiene (4). To a solution of 2.16 g (5.34 mmol) of triphenylmethylphosphonium iodide in 50 mL of anhydrous ether, 3.5 mL (5.3 mmol) of *n*-butyllithium (1.5 M in hexane) was added over 10 min and allowed to stir an additional 10 min. The orange solution was cooled to 0 °C and 1.0 g (2.67 mmol) of 2,2,4,4-tetraphenyl-3-butenaldehyde[11] in 50 mL of anhydrous ether was slowly added over 1 h with vigorous stirring. The mixture was allowed to warm to room temperature and stirred for 7 h. The reaction mixture was poured into cold pentane and filtered through Celite. Neutral workup[27] gave 1.05 g of an orange-red oil. Chromatography on a 80 × 3.0 cm silica gel column eluted with 0.5% ether in hexane with 100-mL fractions being collected gave the following: fractions 11–15, 0.95 g of a colorless oil. The oil was then subjected to preparative HPLC eluted with 0.5% ether and 0.5% acetonitrile in hexane to give the following: peak 1, R_f = 16 min, 0.690 g (1.85 mmol) (69.3%) of pentadiene, mp 79–80 °C, and peak 2, R_f = 20 min, 0.201 g (0.617 mmol) (23.1%) of 1,1,3,3-tetraphenylpropene.

The spectral data for 1,1,3,3-tetraphenyl-1,4-pentadiene (**4**) were the following: ^{1}H NMR ($CDCl_3$, 200 MHz) δ 6.90–7.50 (m, 21 H, arom, vinyl), 6.18 (dd, J = 17.5, 10.0 Hz, 1 H, vinyl), 4.93 (dd, J = 10.0, 2.5 Hz, 1 H, vinyl), 4.51 (dd, J = 17.5, 2.5 Hz, 1 H, vinyl); IR (KBr) 3079, 3054, 3022, 1598, 1490, 1443, 931, 763, 733, 702, 616 cm^{-1}; UV (hexane) λ_{max} 251 nm (ε 18 800); MS m/e 372.1876 (calcd for $C_{29}H_{24}$, m/e 372.1878).

Anal. Calcd for $C_{29}H_{24}$: C, 93.51; H, 6.49. Found: C, 93.54; H, 6.50.

3-Methyl-3-(2,2-dicyanovinyl)-1,1,5,5-tetraphenyl-1,4-pentadiene (5). A mixture of 2.00 g (4.82 mmol) of 2,2-bis(2,2-diphenylvinyl)propionaldehyde,[12] 0.35 g (5.22 mmol) of malonitrile, 0.14 g (1.6 mmol) of β-alanine, and 2 mL of acetic acid in 80 mL of toluene was refluxed for 16 h with a Dean-Stark trap to remove water. Neutral workup[27] afforded 1.84 g of a brown oily solid. Recrystallization from ether/hexane yielded 1.57 g (3.39 mmol) (70.3%) of the triene as a pale yellow solid (mp 111–112 °C).

The spectral data for 3-methyl-3-(2,2-dicyanovinyl)-1,1,5,5-tetraphenyl-1,4-pentadiene (**5**) were the following: ^{1}H NMR ($CDCl_3$, 200 MHz) δ 7.00–7.62 (m, 20 H, arom), 6.75 (s, 1 H, vinyl), 6.08 (s, 2 H, vinyl), 1.70 (s, 3 H, CH_3); IR (KBr) 3058, 3021, 2931, 1598, 1577, 1492, 1444, 775, 761, 704, 694 cm^{-1}; UV (hexane) λ_{max} 252 (ε 23 700), 298 nm (ε 16 500); MS m/e 462.2102 (calcd for $C_{34}H_{26}N_2$, m/e 462.2095).

Anal. Calcd for $C_{34}H_{26}N_2$: C, 88.28; H, 5.67. Found: C, 87.96; H, 5.65.

General Procedure for Exploratory Photolysis. All exploratory irradiations were performed with an immersion well apparatus and a 450-W Hanovia medium-pressure mercury lamp equipped with either a Pyrex (λ > 280 nm) or a Corex (λ > 260 nm) 2-mm filter. All solutions were purged with deoxygenated and dried nitrogen[29] for 1 h prior to and during photolysis. All of the solid-state runs were done under an atmosphere of deoxygenated and dried nitrogen.[29] Solid samples were irradiated as a crystalline film deposited by slow evaporation of a solution in an appropriate solvent on the inside of a Pyrex immersion well cell. The crystalline film was dried by a stream of dry nitrogen for 2 h prior to photolysis. The solid sample was cooled during the photolysis by im-

(27) All reactions were run under nitrogen dried by passage over anhydrous calcium sulfate. Neutral workup refers to dilution with the indicated solvent, successive washing with distilled water and saturated aqueous sodium chloride, drying over anhydrous magnesium sulfate, filtration, and concentration in vacuo. Basic workup included a washing with saturated sodium bicarbonate prior to the water wash. All melting points were determined with a calibrated hot stage apparatus. Elemental analyses were performed by Galbraith Laboratories Inc., Knoxville, TN 37921. Column chromatography was performed on silica gel (Matheson, Coleman, and Bell, grade 62, 60–200 mesh) mixed with 1% (v/v) Sylvania green phosphor slurry-packed into Vycor quartz columns, permitting monitoring with a hand-held ultraviolet lamp. Plates (20 × 20 cm) for preparative thick-layer chromatography (TLC) were prepared with MN-Kieselgel G/UV 254 silica gel. High-performance liquid chromatography (HPLC) was performed on a system incorporating a LDC 5000-psi minipump and a LDC 254-nm detector. For analytical HPLC, a 0.46 × 50 cm polished stainless steel column packed with 4–6 μm porous silica gel beads[28] was employed. For preparative HPLC, a 0.95 × 50 cm polished stainless steel column packed with 8–12 μm porous silica gel beads[28] was employed, with 15–40 mg of sample separated at a time. Hexane used for HPLC elution was purified by stirring with a 1:1 mixture of concentrated nitric acid and concentrated sulfuric acid, followed by successive washing with water until colorless and saturated aqueous sodium bicarbonate and saturated sodium chloride, drying over anhydrous calcium chloride, filtration through alumina, and distillation from calcium hydride. Ethyl acetate used for HPLC was distilled from phosphorus pentoxide. Benzene used in photolysis was purified by successive washing with saturated potassium permanganate in 10% sulfuric acid, water, concentrated sulfuric acid until colorless, water, saturated aqueous sodium bicarbonate, and saturated aqueous sodium chloride, followed by drying over anhydrous calcium chloride, filtration, and distillation from calcium hydride. Tetrahydrofuran (THF) used in reactions was purified by drying over potassium hydroxide, followed by successive distillations from calcium hydride, lithium aluminum hydride, and sodium benzophenone ketyl.

(28) Zimmerman, H. E.; Welter, T. R.; Tartler, D.; Bunce, R. A.; Ramsden, W. D.; King, R. K.; St. Clair, J. D. Unpublished results.

(29) Meites, L.; Meites, T. *Anal. Chem.* **1948**, *20*, 984–985.

(30) Sheldrick, G. M. In *Crystallographic Computing 3*; Sheldrick, G. M., Kruger, C., Goddard, R., Eds.; Oxford University Press: London, 1983; pp 175–189.

(31) Nicolet SHELXTL+, Nicolet Instruments Corp., Madison, WI, 1988.

Table VI. Summary of Crystal Data Collection Parameters[a] for Di-π-methane Reactants

parameter	pentadiene **1**	pentadiene **2**	pentadiene **3**	pentadiene **4**	triene **5**
a axis (Å)	10.505 (0.002)	8.067 (0.003)	6.731 (0.003)	11.421 (0.003)	8.699 (0.003)
b axis (Å)	15.471 (0.003)	18.009 (0.004)	8.986 (0.005)	19.059 (0.005)	17.007 (0.007)
c axis (Å)	14.540 (0.003)	28.680 (0.009)	29.220 (0.001)	19.574 (0.005)	17.566 (0.007)
α angle (deg)	90.00 (0.00)	90.00 (0.00)	90.00 (0.00)	90.00 (0.00)	90.00 (0.00)
β angle (deg)	98.60 (0.002)	90.00 (0.00)	90.00 (0.00)	90.00 (0.00)	90.00 (0.00)
γ angle (deg)	90.00 (0.00)	90.00 (0.00)	90.00 (0.00)	90.00 (0.00)	90.00 (0.00)
vol (Å^3)	2336.5	4166.9	1741.6	4260.5	2609.5
molcules/cell (*Z*)	4	8	4	8	4
density (g/cm^3, calc)	1.20	1.13	1.14	1.16	1.18
temperature (°C)	−30	22	22	22	−30
space group	$P2_1/N$	*Pnaa*	$Pca2_1$	*Pbca*	$P2_12_12_1$
μ (mm^{-1})	0.07	0.06	0.07	0.06	0.06
radiation type	Mo Kα	Mo Kα	Mo Kα	Mo Kα	Mo Kα
scan mode	θ–2θ	ω	ω	ω	ω
2θ limits (deg)	3.5–45.8	4.0–45.8	4.5–45.8	4.0–45.8	4.0–45.8
minimum (*h*,*k*,*l*)	(0,0,−17)	(0,0,0)	(0,0,0)	(0,0,0)	(0,0,0)
maximum (*h*,*k*,*l*)	(13,18,17)	(9,20,32)	(8,10,32)	(13,21,22)	(10,19,20)
scan range (deg)	0.7/0.7	0.6/0.6	1.0/1.0	0.7/0.7	0.8/0.8
measured reflcns	3497	3291	1470	4501	2084
unique reflctns	3148	2866	1339	2922	2062
obsd reflctns	2631	1645	1009	2052	1704
goodness of fit	1.56	1.87	1.51	1.79	1.57
$R_1(F)$	0.043	0.093	0.056	0.062	0.048
$R_w(F)$	0.049	0.088	0.055	0.057	0.051

[a] Standard deviations are given in parentheses.

Table VII. Summary of Crystal Data Collection Parameters[a] for Cyclohexenone Reactants

parameter	cyclohexenone **29a**	cyclohexenone **29b**	cyclohexenone **29c**	cyclohexenone **33**	cyclohexenone **35**
a axis (Å)	9.034 (0.003)	10.469 (0.003)	11.464 (0.004)	19.823 (0.005)	19.879 (0.003)
b axis (Å)	9.784 (0.003)	19.517 (0.006)	11.464 (0.004)	14.133 (0.003)	15.224 (0.004)
c axis (Å)	14.925 (0.006)	10.709 (0.003)	14.038 (0.004)	20.524 (0.004)	12.516 (0.003)
α angle (deg)	90.00 (0.00)	90.00 (0.00)	90.00 (0.00)	90.00 (0.00)	90.00 (0.00)
β angle (deg)	90.00 (0.00)	100.89 (0.02)	90.00 (0.00)	91.01 (0.02)	110.53 (0.02)
γ angle (deg)	90.00 (0.00)	90.00 (0.00)	90.00 (0.00)	90.00 (0.00)	90.00 (0.00)
vol (Å^3)	1319.7	2148.8	1845.1	5749.1	1762.7
molecules/cem (*Z*)	4	4	4	16	4
density (g/cm^3, calc)	1.25	1.24	1.25	1.21	1.22
temperature (°C)	−30	22	−140	22	22
space group	$P2_12_12_1$	$P2_1$	$P4_1$	*C*2/*c*	$P2_10/C$
μ (mm^{-1})	0.07	0.07	0.07	0.07	0.07
radiation type	Mo Kα	Mo Kα	Mo Kα	Mo Kα	Mo Kα
scan mode	ω	ω	ω	ω	θ–2θ
2θ limits (deg)	4.0–48.3	4.0–45.8	4.0–45.8	4.0–45.8	4.0–54.9
minimum (*h*,*k*,*l*)	(0,0.0)	(0,0,−12)	(0,0,0)	(0,0,−23)	(0,0,−17)
maximum (*h*,*k*,*l*)	(13,13,16)	(12,22,12)	(13,13,16)	(22,16,23)	(13,20,17)
scan range (deg)	0.9/0.9	0.8/0.9	0.9/0.9	0.5/0.5	0.8/0.9
reflctns measured	1085	3000	1259	8561	4433
unique reflctns	1068	2798	1134	3956	4041
obsd reflctns	966	1938	1089	2940	3435
goodness of fit	1.65	1.51	4.03	1.96	1.72
$R_1(F)$	0.050	0.070	0.058	0.061	0.054
$R_w(F)$	0.061	0.063	0.059	0.051	0.060

[a] Standard deviations are given in parentheses.

mersion of the photolysis cell in either a room temperature water bath, an ice water bath, or a dry ice/acetone bath.

Exploratory Solid-State Photolysis of 1,1,3,3-Tetraphenyl-5,5-dicyano-1,4-pentadiene (1).[13] A crystalline film of 314 mg (0.744 mmol) of 1,1,3,3-tetraphenyl-5,5-dicyano-1,4-pentadiene, deposited by slow evaporation of a 20% ether in hexane solution, was irradiated at −78 °C for 2.5 h through Pyrex. The resulting orange-red solid was subjected to preparative HPLC eluted with 8% ether and 0.5% acetonitrile in hexane to give the following: peak 1, R_f = 48 min, 227.1 mg (72.3%) of starting diene; and peak 2, R_f = 81 min, 74.8 mg (23.8%) of 7,7-dicyano-9,9,11-triphenyltricyclo[6.3.0.0^{1,6}]undec-2,4,10-triene as a pale purple-red solid. Recrystallization from ether/hexane yielded 69.7 mg (21.6%) of the tricyclic compound as a white solid (mp 125–128 °C dec).

The spectral data for 7,7-dicyano-9,9,11-triphenyltricyclo[6.3.0.0^{1,6}]-undec-2,4,10-triene (**25**) were the following: ^{1}H NMR ($CDCl_3$, 200 MHz) δ 7.10–7.82 (m, 16 H, arom, vinyl), 6.28 (m, 1 H, vinyl), 5.93 (m, 2 H, vinyl), 5.45 (d, *J* = 10.0 Hz, 1 H, vinyl), 4.60 (s, 1 H, CH), 3.80 (br s, 1 H, CH); IR (KBr) 3032, 3025, 2923, 2243, 1599, 1493, 1447, 1033, 759, 717, 702, 697 cm^{-1}; MS *m*/*e* 422.1772 (calcd for $C_{31}H_{22}N_2$, *m*/*e* 422.1778).

Anal. Calcd for $C_{31}H_{22}N_2$: C, 88.11; H, 5.25. Found: C, 88.21; H, 5.30.

Exploratory Solid-State Photolysis of 1,1-Diphenyl-3,3-diisopropyl-5,5-dicyano-1,4-pentadiene (2).[2] In an NMR tube, 15.2 mg (0.0429 mmol) of crystalline (needles from hexane) 1,1-diphenyl-3,3-diisopropyl-5,5-dicyano-1,4-pentadiene was irradiated under deoxygenated and dried nitrogen at −78 °C for 2 h through Pyrex. The resulting yellow solid was subjected to HPLC eluted with 5% ether and 1% acetonitrile in hexane to give the following: peak 1, R_f = 17 min, 7.9 mg (52.0%) of 7,7-dicyano-9,9-diisopropyl-11-phenyltricyclo[6.3.0.0^{1,6}]undec-2,4,10-triene (mp 139–140 °C dec) as a white solid; and peak 2, R_f = 22 min, 7.1 mg (46.7%) of starting diene.

The spectral data for 7,7-dicyano-9,9-diisopropyl-11-phenyltricyclo-[6.3.0.0^{1,6}]undec-2,4,10-triene (**26**) were the following: ^{1}H NMR ($CDCl_3$, 200 MHz) δ 7.25–7.60 (m, 5 H, arom), 6.33 (m, 1 H, vinyl), 5.96 (m, 3 H, vinyl), 5.68 (d, *J* = 10.0 Hz, 1 H, vinyl), 3.94 (s, 1 H, CH), 3.85 (br s, 1 H, CH), 2.81 (sept, *J* = 7.0 Hz, 1 H, CH), 1.75 (sept, *J* = 7.0 Hz, 1 H, CH), 1.30 (d, *J* = 7.0 Hz, 6 H, CH), 1.24 (d, *J* = 7.0 Hz, 6 H, CH); IR (KBr) 2967, 2946, 2930, 2238, 1496, 1469, 1373, 766, 711, 790 cm^{-1}; MS *m*/*e* 354.2109 (calcd for $C_{25}H_{26}N_2$, *m*/*e* 354.2096).

Anal. Calcd for $C_{25}H_{26}N_2$: C, 84.71; H, 7.39. Found: C, 84.82; H, 7.42.

Exploratory Solid-State Photolysis of 1,1-Diphenyl-3,3-dimethyl-5,5-dicyano-1,4-pentadiene (3).[15] A crystalline film of 210 mg (0.704 mmol)

Table VIII. Summary of Crystal Data Collection Parameters[b] for Photoproducts of 3-Methyl-3-(2,2-dicyanovinyl)-1,1,5,5-tetraphenyl-1,4-pentadiene (**5**)

parameter	cyclopropane **22**	cyclopropane **23**	cyclopropane **24T**	cyclopropane **24C**	cyclopentene **28**
a axis (Å)	8.439 (0.001)	9.702 (0.002)	10.451 (0.004)	9.003 (0.002)	9.676 (0.002)
b axis (Å)	36.514 (0.003)	16.234 (0.004)	13.165 (0.005)	10.738 (0.002)	15.651 (0.004)
c axis (Å)	10.379 (0.001)	16.455 (0.003)	10.534 (0.005)	14.136 (0.003)	17.666 (0.005)
α angle (deg)	90.00 (0.00)	90.00 (0.00)	90.00 (0.00)	74.64 (0.01)	72.85 (0.02)
β angle (deg)	90.00 (0.00)	90.00 (0.00)	112.29 (0.03)	80.88 (0.01)	86.88 (0.02)
γ angle (deg)	90.00 (0.00)	90.00 (0.00)	90.00 (0.00)	85.32 (0.01)	81.24 (0.02)
vol (Å^3)	1318.1	2591.8	1341.1	1300.1	2526.4
molecules/cell (*Z*)	8	4	2	2	4
density (g/cm^3, calc)	1.20	1.19	1.15	1.18	1.21
temperature (°C)	22	22	22	22	−140
space group	*Pbca*	$P2_12_12_1$	$P2_1$	$P\bar{1}$	$P\bar{1}$
μ (mm^{-1})	0.6	0.48	0.48	0.49	0.07
radiation type	Cu Kα	Cu Kα	Cu Kα	Cu Kα	Mo Kα
scan mode	ω	ω	ω	ω	ω
2θ limits (deg)	4.0–45.7	4.0–115.0	4.0–115.0	4.0–115.0	4.0–45.8
minimum (*h*,*k*,*l*)	(0,−12,−17)	(0,0,0)	(−20,0,0)	(0,−12,−16)	(0,−18,−20)
maximum (*h*,*k*,*l*)	(11,12,17)	(11,18,19)	(20,13,24)	(10,12,16)	(11,18,20)
scan range (deg)	0.9/0.9	0.7/0.7	0.9/0.9	0.6/0.6	0.5/0.5
reflctns measured	2488	2042	2061	3817	6129
unique reflctns	2120	2019	1936	3546	5645
obsd reflctns	1213	2761	1211	2994	4367
goodness of fit	1.58	1.38	*a*	1.70	1.45
$R_1(F)$	0.075	0.045		0.047	0.053
$R_w(F)$	0.068	0.049		0.056	0.055

[a] This structure is highly disordered, and refinement is still in progress. [b] Standard deviations are given in parentheses.

Table IX. Summary of Crystal Data and Intensity Collection Parameters[a] for Pentenol **42** and Solid-State Photoproducts from Di-π-methane Reactants **1** and **2** and Triphenylcyclohenenone **35**

parameter	pentenol **42**	tricyclic **25**	tricyclic **26**	bicyclic ketone **39**	bicyclic ketone **40**
a axis (Å)	13.088 (0.003)	12.188 (0.002)	12.206 (0.004)	8.668 (0.001)	9.534 (0.002)
b axis (Å)	10.286 (0.003)	10.356 (0.003)	11.898 (0.002)	9.887 (0.002)	11.805 (0.003)
c axis (Å)	17.661 (0.007)	18.647 (0.004)	14.988 (0.004)	21.204 (0.005)	16.217 (0.003)
α angle (deg)	90.00 (0.00)	90.00 (0.00)	90.00 (0.00)	90.00 (0.00)	103.69 (0.02)
β angle (deg)	99.22 (0.03)	107.48 (0.01)	107.93 (0.02)	100.65 (0.02)	98.19 (0.02)
γ angle (deg)	90.00 (0.00)	90.00 (0.00)	90.00 (0.00)	90.00 (0.00)	90.90 (0.02)
vol (Å^3)	2346.9	2186.8	2071.0	1785.9	1752.6
molecules/cell (*Z*)	4	4	4	4	4
density (g/cm^3, calc)	1.19	1.20	1.14	1.21	1.18
temperature (°C)	22	22	22	22	22
space group	$P2_1/N$	$P2_1$	$P2_1/N$	$P2_1/N$	$P\bar{1}$
μ (mm^{-1})	0.06	0.53	0.47	0.07	0.43
radiation type	Mo Kα	Cu Kα	Cu Kα	Mo Kα	Cu Kα
scan mode	θ–2θ	ω	ω	θ–2θ	ω
2θ limits	4.0–54.9	4.0–115.0	4.0–115.0	4.0–54.9	4.0–115.0
minimum (*h*,*k*,*l*)	(0,0,−23)	(0,0,−21)	(0,0,−17)	(0,0,−28)	(0,−13,−18)
maximum (*h*,*k*,*l*)	(17,14,23)	(14,12,21)	(14,14,17)	(12,13,18)	(11,13,18)
scan range (deg)	0.8/0.8	1.0/1.0	0.5/0.5	0.9/0.9	0.6/0.6
reflctns measured	5955	3471	3149	4636	5142
unique reflctns	5408	3290	2818	4108	4801
obsd reflctns	5408	3076	2371	3217	4195
goodness of fit	1.79	2.44	2.16	2.09	2.80
$R_1(F)$	0.054	0.056	0.054	0.056	0.046
$R_w(F)$	0.062	0.076	0.067	0.067	0.050

[a] Standard deviations are given in parentheses.

of 1,1-diphenyl-3,3-dimethyl-5,5-dicyano-1,4-pentadiene, deposited by slow evaporation of a 20% ether in hexane solution, was irradiated at 0 °C for 16 h through Pyrex. The resulting white solid was determined to be unreacted starting diene by HPLC and ^{1}H NMR.

Exploratory Solution Photolysis of 1,1,3,3-Tetraphenyl-1,4-pentadiene (4). A solution of 249 mg (0.914 mmol) of 1,1,3,3-tetraphenyl-1,4-pentadiene in 500 mL of benzene was irradiated through Pyrex for 4 h. Concentration in vacuo yielded 255 mg of a yellow oil which was subjected to preparative HPLC eluted with 1% ether and 1% acetonitrile in hexane to give the following: peak 1, R_f = 14 min, 75.4 mg (30.3%) of 1,1,2,2-tetraphenyl-3-vinylcyclopropane as a white solid (mp 127–129 °C); peak 2, R_f = 17 min, 98.8 mg (39.7%) of *trans*-1,1,2,3-tetraphenyl-2-vinylcyclopropane (mp 165–167 °C); and peak 3, R_f = 22 min, 65.4 mg (26.3%) of the starting diene.

The spectral data for 1,1,2,2-tetraphenyl-3-vinylcyclopropane (**19**) were the following: ^{1}H NMR ($CDCl_3$, 200 MHz) δ 7.5 (dd, J = 8.0, 2.0 Hz, 4 H, arom) 6.9–7.25 (m, 16 H, arom), 5.58 (m, 2 H, vinyl), 5.21 (m, 1 H, vinyl), 3.46 (m, 1 H, CH); IR (KBr) 3010, 2958, 2899, 1595, 1497, 1374, 1072, 850, 805, 732, 702 cm^{-1}; MS *m/e* 372.1891 (calcd for $C_{29}H_{24}$, *m/e* 372.1878).

Anal. Calcd for $C_{29}H_{24}$: C, 93.51; H, 6.49. Found: C, 93.40; H, 6.47.

The spectral data for *trans*-1,1,2,3-tetraphenyl-2-vinylcyclopropane (**20**) were the following: ^{1}H NMR ($CDCl_3$, 200 MHz) δ 7.48 (dd, J = 8.0, 2.0 Hz, 4 H arom), 6.90–7.33 (m, 16 H, arom), 6.11 (dd, J = 17.0, 10.0 Hz, 1 H, vinyl), 5.03 (dd, J = 10.0, 2.0 Hz, 1 H, vinyl), 4.51 (dd, J = 17.0, 2.0 Hz, 1 H, vinyl), 3.94 (s, 1 H, CH); IR (KBr) 3010, 2959, 2898, 1597, 1494, 1440, 1370, 1072, 855, 734, 705 cm^{-1}; MS *m/e* 372.1893 (calcd for $C_{29}H_{24}$, *m/e* 372.1878).

Anal. Calcd for $C_{29}H_{24}$: C, 93.51; H, 6.49. Found: C, 93.80; H, 6.48.

Exploratory Sensitized Solution Photolysis of 1,1,3,3-Tetraphenyl-1,4-pentadiene (4). A solution of 20.1 mg (0.054 mmol) of 1,1,3,3-tetraphenyl-1,4-pentadiene and 28 mL of 0.3 M acetophenone in benzene was irradiated using the microoptical bench apparatus[32] at 325 nm for 3.5 h. Concentration in vacuo yielded 21.5 mg of a white solid. Analysis by ^{1}H NMR revealed the presence of starting material and 1,1,2,2-

(32) Zimmerman, H. E. *Mol. Photochem.* **1971**, *3*, 281–292.

Table X. Summary of Crystal Data and Intensity Collection Parameters[a] for Housane **16** and Vinylcyclopropane **17**

parameter	housane **16**	cyclopropane **17**
a axis (Å)	22.527 (0.005)	11.289 (0.002)
b axis (Å)	9.864 (0.002)	16.317 (0.003)
c axis (Å)	19.772 (0.004)	12.943 (0.002)
α angle (deg)	90.00 (0.00)	90.00 (0.00)
β angle (deg)	130.09 (0.02)	93.94 (0.01)
γ angle (deg)	90.00 (0.00)	90.00 (0.00)
vol (Å^3)	3361.3	2378.6
molecules/cell (Z)	8	4
density (g/cm^3, calc)	1.18	1.12
temperature (°C)	22	22
space group	$C2/C$	$P2_1/C$
μ (mm^{-1})	0.50	0.44
radiation type	Cu Kα	Cu Kα
scan mode	ω	ω
2θ limits (deg)	3.5–115.0	4.0–115.0
minimum (h,k,l)	(0,0,–22)	(0,0,–15)
maximum (h,k,l)	(25,11,22)	(13,18,15)
scan range (deg)	0.7/0.7	0.7/0.7
reflctns measured	2541	3590
unique reflctns	2302	3246
obsd reflctns	2071	2035
goodness of fit	3.19	1.32
$R_1(F)$	0.045	0.092
$R_W(F)$	0.051	0.111

[a] Standard deviations are given in parentheses.

Table XI. Conditions Employed in the Solution Quantum Yield Determination for 3-Methyl-3-(2,2-dicyanovinyl)-1,1,5,5-tetraphenyl-1,4-pentadiene and Summary of Results

run no.	reactant[a]	light abs,[b] μEinsteins	% conv	mmol of photoproduct formed × 10^3 **24C**	**22**	**24T**	**23**
1	0.0181	27.17	23.2	1.158	1.270	0.991	0.781
2	0.0185	7.42	8.76	0.335	0.383	0.338	0.205
3	0.0277	37.13	22.3	1.982	1.564	1.498	1.129

[a] Runs performed in 40 mL of benzene. [b] Light absorbed, irradiated at 313 nm.

tetraphenyl-3-vinylcyclopropane (**19**).

Exploratory Solid-State Photolysis of 1,1,3,3-Tetraphenyl-1,4-pentadiene (4). A crystalline film of 248 mg (0.666 mmol) of 1,1,3,3-tetraphenyl-1,4-pentadiene, deposited by slow evaporation of an anhydrous ether solution, was irradiated at −78 °C for 16 h through Pyrex. The resulting white solid was subjected to preparative HPLC eluted with 1% ether and 1% acetonitrile in hexane to give the following: peak 1, R_f = 14 min, 110.0 mg (44.3%) of 1,1,3,3-tetraphenylvinylcyclopropane (**19**); and peak 2, R_f = 22 min, 127.1 mg (51.2%) of starting pentadiene.

Ozonolysis of 1,1,2,2-Tetraphenyl-3-vinylcyclopropane (19). A solution of 12.3 mg (0.033 mmol) of 1,1,2,2-tetraphenyl-3-vinylcyclopropane in methylene chloride at −78 °C was purged with ozone for 5 min. The solution was then purged with nitrogen for 30 min and 0.50 mL of dimethyl sulfide was added. The mixture was warmed to 0 °C and stirred for 3 h. Concentration in vacuo yielded 13.2 mg of a colorless oil. Crystallization from hexane gave 10.2 mg (82.5%) of a white solid (mp 206–207 °C). Spectral data were consistent with 1,1,2,2-tetraphenylcyclopropanecarboxaldehyde (**21**).[11]

Ozonolysis of *trans*-1,1,2,3-tetraphenyl-2-vinylcyclopropane (20). A solution of 27.4 mg (0.0735 mmol) of 1,1,2,3-tetraphenyl-2-vinylcyclopropane in methylene chloride at −78 °C was purged with ozone for 5 min. The solution was then purged with nitrogen for 30 min and 0.50 mL of dimethyl sulfide was added. The mixture was warmed to 0 °C and stirred for 3 h. Concentration in vacuo yielded 28.2 mg of a colorless oil. Crystallization from hexane gave 23.3 mg (84.7%) of a white solid (mp 156–157 °C). Spectral data were consistent with *trans*-1,2,2,3-tetraphenylcyclopropanecarboxaldehyde (**18**).[11]

Exploratory Solution Photolysis of 3-Methyl-3-(2,2-dicyanovinyl)-1,1,5,5-tetraphenyl-1,4-pentadiene (5). A solution of 147.7 mg (0.319 mmol) of 3-methyl-3-(2,2-dicyanovinyl)-1,1,5,5-tetraphenyl-1,4-pentadiene in 165 mL of benzene was irradiated through Pyrex for 4 h. Concentration in vacuo yielded 162 mg of an orange oil that was subjected to preparative HPLC eluted with 2% ether, 2% ethyl acetate, and 2% acetonitrile in pentane to give the following: peak 1, R_f = 22 min, 28.1 mg (19.0%) of *cis*-1,1-diphenyl-2-methyl-2-(2,2-dicyanovinyl)-3-(2,2-diphenylvinyl)cyclopropane; peak 2, R_f = 28 min, 42.5 mg (28.8%) of *trans*-1,1-dicyano-2-methyl-2,3-bis(2,2-diphenylvinyl)cyclopropane; peak 3, R_f = 46 min, 12.1 mg (8.2%) of *trans*-1,1-diphenyl-2-methyl-2-(2,2-dicyanovinyl)-3-(2,2-diphenylvinyl)cyclopropane; and peak 4, R_f = 50 min, 31.1 mg (21.1%) of *trans*-1,1-diphenyl-2-methyl-2-(2,2-diphenylvinyl)-3-(2,2-dicyanovinyl)cyclopropane.

Table XII. Solution Quantum Yields for Formation of the Photoproducts of 3-Methyl-3-(2,2-dicyanovinyl)-1,1,5,5-tetraphenyl-1,4-pentadiene (**5**)

run no.	quantum yield **24C**	**22**	**24T**	**23**
1	0.0467	0.0426	0.0365	0.0288
2	0.0533	0.0421	0.0403	0.0304
3	0.0452	0.0516	0.0456	0.0276

The spectral data for *cis*-1,1-diphenyl-2-methyl-2-(2,2-dicyanovinyl)-3-(2,2-diphenylvinyl)cyclopropane (**24C**) were the following: ^{1}H NMR ($CDCl_3$, 200 MHz) δ 6.95–7.49 (m, 20 H, arom and 1 H vinyl), 5.86 (d, J = 9.5 Hz, 1 H, vinyl), 2.82 (d, J = 9.5 Hz, 1 H, CH), 1.33 (s, 3 H, CH_3); IR (KBr) 3057, 3027, 2929, 2232, 1587, 1494, 1447, 941, 764, 748, 705 cm^{-1}; MS m/e 462.2111 (calcd for $C_{34}H_{26}N_2$, m/e 462.2089).

Anal. Calcd for $C_{34}H_{26}N_2$: C, 88.28; H, 5.67. Found: C, 88.10; H, 5.60.

The spectral data for *trans*-1,1-dicyano-2-methyl-2,3-bis(2,2-diphenylvinyl)cyclopropane (**22**) were the following: ^{1}H NMR ($CDCl_3$, 200 MHz) δ 7.00–7.50 (m, 20 H, arom), 6.35 (s, 1 H, vinyl), 5.51 (d, J = 9.5 Hz, 1 H, vinyl), 2.32 (d, J = 9.5 Hz, 1 H, CH), 1.65 (s, 3 H, CH_3); IR (KBr) 3056, 3025, 1599, 1577, 1494, 1445, 1075, 1062, 1031, 766, 732, 698 cm^{-1}; MS m/e 462.2111 (calcd for $C_{34}H_{26}N_2$, m/e 462.2093).

Anal. Calcd for $C_{34}H_{26}N_2$: C, 88.28; H, 5.67. Found: C, 88.13; H, 5.74.

The spectral data for *trans*-1,1-diphenyl-2-methyl-2-(2,2-dicyanovinyl)-3-(2,2-diphenylvinyl)cyclopropane (**24T**) were the following: ^{1}H NMR ($CDCl_3$, 200 MHz) δ 6.9–7.50 (m, 20 H, arom), 6.09 (s, 1 H, vinyl), 5.71 (d, J = 9.5 Hz, 1 H, vinyl), 2.92 (d, J = 9.5 Hz, 1 H, CH), 1.41 (s, 3 H, CH_3); IR (KBr) 3057, 3027, 2925, 2232, 1583, 1494, 1447, 1075, 1028, 767, 700 cm^{-1}; MS m/e 462.2111 (calcd for $C_{34}H_{26}N_2$, m/e 462.2101).

Anal. Calcd for $C_{34}H_{26}N_2$: C, 88.28; H, 5.67. Found: C, 88.36; H, 5.68.

The spectral data for *trans*-1,1-diphenyl-2-methyl-2-(2,2-diphenylvinyl)-3-(2,2-dicyanovinyl)cyclopropane (**23**) were the following: ^{1}H NMR ($CDCl_3$, 200 MHz) δ 6.95–7.50 (m, 20 H, arom), 6.63 (d, J = 9.5 Hz, 1 H, vinyl), 6.05 (s, 1 H, vinyl), 2.75 (d, J = 9.5 Hz, 1 H, CH), 1.57 (s, 3 H, CH_3); IR (KBr) 3058, 3027, 2925, 2232, 1597, 1582, 1494, 1447, 771, 706 cm^{-1}; MS m/e 462.2111 (calcd for $C_{34}H_{26}N_2$, m/e 462.2090).

Anal. Calcd for $C_{34}H_{26}N_2$: C, 88.28; H, 5.67. Found: C, 88.59; H, 5.47.

Exploratory Sensitized Solution Photolysis of 3-Methyl-3-(2,2-dicyanovinyl)-1,1,5,5-tetraphenyl-1,4-pentadiene (5). A solution of 8.5 mg (0.018 mmol) of 3-methyl-3-(2,2-dicyanovinyl)-1,1,5,5-tetraphenyl-1,4-pentadiene and 2 mL of acetophenone in 27 mL of benzene was irradiated using the microoptical bench apparatus at 325 nm for 2 h. Concentration in vacuo yielded 9.1 mg of a pale yellow oil. Analysis by ^{1}H NMR revealed starting material, divinylcyclopropane **23**, and an unidentified product with a ^{1}H NMR indicative of a divinylcyclopropane: ^{1}H NMR ($CDCl_3$, 200 MHz) δ 6.63 (s, 1 H), 6.24 (d, J = 12 Hz, 1 H), 2.78 (d, J = 12 Hz, 1 H), 1.41 (s, 1 H).

Exploratory Solid-State Photolysis of 3-Methyl-3-(2,2-dicyanovinyl)-1,1,5,5-tetraphenyl-1,4-pentadiene (5). A crystalline film deposited by slow evaporation of a hexane solution was irradiated at −78 °C for 8 h through Pyrex. The resulting yellow solid was subjected to preparative HPLC eluted with 4% ether and 1% acetonitrile in hexane to give the following: peak 1, R_f = 35 min, 51.8 mg (21.4%) of 1-methyl-3,3,4,4-tetraphenyl-5-(3,3-dicyanovinyl)-1-cyclopentene (mp 137–138 °C); and peak 2, R_f = 53 min, 174.0 mg (71.9%) of starting triene.

The spectral data for 1-methyl-3,3,4,4-tetraphenyl-5-(3,3-dicyanovinyl)-1-cyclopentene (**28**) were the following: ^{1}H NMR ($CDCl_3$, 200 MHz) δ 6.86–7.40 (m, 18 H, arom), 6.63 (m, 2 H, arom), 6.55 (br s, 1 H, vinyl), 6.43 (d, J = 11.0 Hz, 1 H, vinyl), 4.99 (br d, J = 11.0 Hz, 1 H, vinyl), 1.88 (s, 3 H, CH_3); IR (KBr) 3056, 3035, 2925, 2234, 1598, 1492, 1444, 1035, 756, 705 cm^{-1}; MS m/e 462.2111 (calcd for $C_{34}H_{26}N_2$, m/e 462.2096).

Anal. Calcd for $C_{34}H_{26}N_2$: C, 88.28; H, 5.67. Found: C, 88.54; H, 5.63.

Table XIII. Conditions Employed in the Solution Quantum Yield Determination for 1,1,3,3-Tetraphenyl-1,4-pentadiene (**4**) and Summary of Results

run no.	reactant,[a] mmol	light abs,[b] μEinsteins	% conv	photoproduct, mmol × 10^3		quantum yield	
				19	**20**	**19**	**20**
1	0.1823	30.54	2.21	1.784	2.246	0.0584	0.0735
2	0.1278	57.22	5.96	3.259	4.352	0.0570	0.0761
3	0.1267	71.70	7.36	3.910	5.410	0.0545	0.0755

[a] Runs performed in 40 mL of acetonitrile. [b] Irradiated at 302 nm.

Table XIV. Crystalline-State Quantum Yield Summary for 1,1,3,3-Tetraphenyl-1,4-pentadiene (**4**)

run no.	reactant, mmol × 10^3	light abs,[a] μEinsteins	product,[b] mmol × 10^3	% conv	quantum yield **19**
1	26.04	79.10	1.316	5.06	0.0166
2	32.75	62.69	1.001	3.06	0.0160
3	26.04	45.91	0.744	2.86	0.0162

[a] Light absorbed, irradiated at 302 nm. [b] Analyzed by ^{1}H NMR.

Exploratory Solid-State Photolysis of 4,4-Diphenylcyclohexenone (29a).[16] A crystalline film of 312 mg (1.26 mmol) of 4,4-diphenylcyclohex-2-en-1-one, deposited by slow evaporation of a hexane solution, was irradiated at 0 °C for 24 h through Pyrex. The resulting pale yellow solid was chromatographed on a 2.5 × 50 cm silica gel column eluted with 6 L of 5% ether in hexane, with 45-mL fractions being collected to give the following: fractions 51–58, 7.1 mg (2.3%) of *trans*-5,6-diphenylbicyclo[3.1.0]hexan-2-one as a white solid (mp 73–74 °C); fractions 76–105, 305 mg (97.8%) of the starting enone as a white solid.

Exploratory Solid-State Photolysis of 4,4-Dibiphenylcyclohexenone (29b).[17] A crystalline film of 62.7 mg (0.157 mmol) of 4,4-dibiphenylcyclohexenone, deposited by slow evaporation of a hexane solution, was irradiated at −78 °C for 1 h through Pyrex. The resulting pale yellow solid was chromatographed on a 1.7 × 89 cm silica gel column eluted with 4.3 L of hexane, 0.5 L of 1% ether in hexane, and 3.2 L of 2% ether in hexane, collecting 42-mL fractions to give the following: fractions 84–103, 9.1 mg (14.6%) of *trans*-5,6-dibiphenylbicyclo[3.1.0]-hexan-2-one as a white solid: fractions 104–123, 51.9 mg (82.8%) of starting enone.

Exploratory Solid-State Photolysis of 4,4-Di(1-naphthyl)cyclohexenone (29c).[18] A crystalline film of 60.0 mg (0.172 mmol) of 4,4-di(1-naphthyl)cyclohex-2-en-1-one deposited by slow evaporation of a hexane solution, was irradiated at −78 °C for 1 h through Pyrex. The resulting white solid was subjected to preparative HPLC eluted with 10% ethyl acetate in hexane to give the following: peak 1, R_f = 15 min, 10.5 mg (17.4%) of *trans*-5,6-di-1-naphthylbicyclo[3.1.0]hexan-2-one as a white solid; peak 2, R_f = 22 min, 49.2 mg (82.1%) of starting cyclohexenone.

Exploratory Solid-State Photolysis of 4,5,5-Triphenylcyclohexenone (35).[19] A crystalline film of 60.0 mg (0.185 mmol) of 4,5,5-triphenylcyclohexenone, deposited by slow evaporation of an ether solution, was irradiated at 0 °C for 16 h through Pyrex. The resulting yellow solid was subjected to preparative HPLC eluted with 2% ethyl acetate and 0.5% acetonitrile in hexane to give the following: peak 1, R_f = 91 min, 3.7 mg (6.2%) of *endo*-6,7-benzo-1,8-diphenylbicyclo[3.2.1]oct-6-en-3-one as a white solid, mp 114–115 °C; peak 2, R_f = 96 min, 15.3 mg (25.5%) of *endo*-4,4,6-triphenylbicyclo[3.1.0]hexan-2-one as a white solid, mp 145–145.5 °C; and peak 3, R_f = 123 min, 37.6 mg (62.7%) of starting enone.

The spectral data for *endo*-4,4,6-triphenylbicyclo[3.1.0]hexan-2-one (**39**) were the following: ^{1}H NMR ($CDCl_3$, 200 MHz) δ 7.68–7.50 (m, 15 H, arom), 3.18 (dd, J = 5.0, 8.5 Hz, 1 H, CH), 3.01 (t, J = 8.5 Hz, 1 H, CH), 2.70 (dd, J = 5.0, 8.5 Hz, 1 H, CH), 2.41 (d, J = 17.5 Hz, 1 H, CH_2), 2.17 (d, J = 17.5 Hz, 1 H, CH_2); IR (KBr) 3055, 3050, 1727, 1491, 1445, 1416, 1184, 1014, 776, 700 cm^{-1}; MS m/e 324.1509 (calcd for $C_{24}H_{20}O$, m/e 324.1514).

Anal. Calcd for $C_{24}H_2O$: C, 88.85; H, 6.21. Found:, C, 88.48; H, 6.32.

The spectral data for *endo*-4,4,6-triphenylbicyclo[3.1.0]hexan-2-one (**40**) were the following: ^{1}H NMR ($CDCl_3$, 200 MHz) δ 6.60–7.50 (m, 14 H, arom), 4.43 (d, J = 5.0 Hz, 1 H, CH), 4.13 (m, J = 5.0 Hz, 1 H, CH), 3.28 (d, J = 17.5 Hz, 1 H, CH_2), 2.98 (d, J = 17.5 Hz, 1 H, CH_2), 2.80 (dd, J = 17.5, 5.0 Hz, 1 H, CH_2), 2.48 (d, J = 17.5 Hz, 1 H, CH_2); IR (KBr) 3059, 3030, 2961, 2923, 1710, 1107, 1081, 1034, 1014, 756, 702 cm^{-1}; MS m/e 324.1507 (calcd for $C_{24}H_{20}O$, m/e 324.1514).

Anal. Calcd for $C_{24}H_{20}O$: C, 88.85; H, 6.21. Found: C, 88.49; H, 6.28.

Exploratory Solid-State Photolysis of 4-Methyl-5,5-diphenylcyclohexenone (33).[19] A crystalline film of 50.1 mg (0.191 mmol) of 4-methyl-5,5-diphenylcyclohexenone, deposited by slow evaporation of a hexane solution, was irradiated at 0 °C for 24 h through Pyrex. The resulting white solid was determined to be unreacted starting enone by HPLC and ^{1}H NMR.

Exploratory Solid-State Photolysis of 1,1,5,5-Tetraphenyl-3,3-dimethylpent-1-en-5-ol (42).[20] A crystalline film of 150.0 mg (0.358 mmol) of 1,1,5,5-tetraphenyl-3,3-dimethylpent-1-en-5-ol, deposited by slow evaporation of an ether solution, was irradiated at −78 °C for 16 h through Corex. The resulting white solid was subjected to preparative HPLC eluted with 5% ether in hexane to give the following: peak 1, R_f = 16 min, 38.5 mg (25.7%) of 4,4-dimethyl-2,2,6,6-tetraphenyltetrahydropyran; peak 2, R_f = 18 min, 36.2 mg (24.1%) of 3,3-dimethyl-2-diphenylmethyl-5,5-diphenyltetrahydrofuran; and peak 3, R_f = 32 min, 69.8 mg (46.6%) of starting pentenol.

The spectral data for 4,4-dimethyl-2,2,6,6-tetraphenyltetrahydropyran (**44**) were the following: ^{1}H NMR ($CDCl_3$, 200 MHz) δ 7.05–7.50 (m, 20 H, arom), 2.35 (s, 4 H, CH_2), 0.51 (s, 6 H, CH_3), IR (KBr) 2953, 2928, 1447, 1210, 1134, 1065, 1014, 753, 746, 732, 704, 695, 609 cm^{-1}; MS m/e 341.1090 (−Ph) (calcd for $C_{31}H_{30}O$, m/e 418.2297).

Anal. Calcd for $C_{31}H_{30}O$: C, 88.95; H, 7.22. Found: C, 88.92; H, 7.26.

The spectral data for 3,3-dimethyl-2-(diphenylmethyl)-5,5-diphenyltetrahydrofuran (**45**) were the following: ^{1}H NMR ($CDCl_3$, 200 MHz) δ 7.00–7.60 (m, 20 H, arom), 4.48 (d, J = 10.5 Hz, 1 H, CH), 4.16 (d, J = 10.5 Hz, 1 H, CH), 2.70 (d, J = 6.0 Hz, 1 H, CH_2), 2.62 (d, J = 6.0 Hz, 1 H, CH_2), 0.92 (s, 3 H, CH_3), 0.51 (s, 3 H, CH_3); IR (KBr) 3059, 3025, 2957, 2917, 2849, 1598, 1494, 1450, 1073, 1032, 755, 702 cm^{-1}; MS m/e 341.1998 (−Ph), 252.1521 (−C(Ph)$_2$) (calcd for $C_{31}H_{30}O$, m/e 418.2297).

Anal. Calcd for $C_{31}H_{30}O$: C, 88.95; H, 7.22. Found: C, 88.61; H, 7.54.

4,4-Dimethyl-2,2,6,6-tetraphenyltetrahydropyran (44). A suspension of 0.592 g (1.36 mmol) of 3,3-dimethyl-1,1,5,5-tetraphenyl-1,5-pentanediol[21] in 100 mL of 6 M HCl was stirred vigorously at room temperature for 16 h. Extraction with ether followed by basic workup[27] yielded 0.558 g of a colorless oil that was chromatographed on a 4 × 67 cm silica gel column eluted with 1 L of hexane and 2 L of 5% ether in hexane, with 250-mL fractions being collected to give the following: fractions 7–9, 0.548 g of 4,4-dimethyl-2,2,6,6-tetraphenyltetrahydropyran as a clear oil. Crystallization from hexane yielded 0.542 g (1.30 mmol) (95.6%) of 4,4-dimethyl-2,2,6,6-tetraphenyltetrahydropyran as white needles, mp 149–150 °C (lit.[21] mp 149 °C).

3,3-Dimethyl-1,1,5,5-tetraphenyl-1,4-pentanediol (47). To a solution of 0.1034 g (0.247 mmol) of 1,1,5,5-tetraphenyl-3,3-dimethylpent-1-en-5-ol and 3 mg (0.075 mmol) of sodium borohydride in THF at 0 °C was added slowly with stirring 0.012 mL (0.095 mmol) of boron trifluoride etherate in 2 mL of THF. The mixture was stirred for 2 h with warming to room temperature and then cooled to 0 °C, 0.5 mL of water added, and the mixture was stirred for 1 h. To the mixture, 0.5 mL of 10% aqueous sodium hydroxide and 0.5 mL of 30% aqueous hydrogen peroxide were added, and the mixture was stirred for 2 h. Neutral workup[27] yielded 0.1120 g of a colorless oil. Preparative TLC eluted twice with 20% ether in hexane gave the following: band 1, 25 mg (0.0574 mmol) (23.0%) of 3,3-dimethyl-1,1,5,5-tetraphenyl-1,5-pentanediol;[12] band 2, 60.0 mg (0.138 mmol) (55.7%) of 3,3-dimethyl-1,1,5,5-tetraphenyl-1,4-pentanediol.

The spectral data for 3,3-dimethyl-1,1,5,5-tetraphenyl-1,4-pentanediol (**47**) were the following: ^{1}H NMR ($CDCl_3$, 200 MHz) δ 7.05–7.55 (m, 20 H, arom), 4.90 (s, 1 H, OH), 4.43 (d, J = 7.5 Hz, 1 H, CH), 4.30 (d, J = 7.5 Hz, 1 H, CH), 2.75 (d, J = 15 Hz, 1 H, CH), 2.65 (s, 1 H, OH), 2.38 (d, J = 15 Hz, 1 H, CH), 0.75 (s, 3 H, CH_3), 0.43 (s, 3 H, CH_3); IR (KBr) 3595, 3405, 3059, 3029, 1585, 1453, 1045, 1020, 759, 710 cm^{-1}; MS m/e 436.2389 (calcd for $C_{31}H_{32}O$, m/e 436.2394).

Anal. Calcd for $C_{31}H_{32}O_2$: C, 85.28; H, 7.39. Found: C, 85.36; H, 7.44.

3,3-Dimethyl-2-(diphenylmethyl)-5,5-diphenyltetrahydrofuran (45). A

Table XV. Crystalline-State Quantum Yield Summary for 4,4-Dibiphenylcyclohexenone (29b)

run no.	reactant, mmol × 10^3	light abs,[a] μEinsteins	% conv	photoproduct,[b] mmol × 10^3		quantum yield	
				30b	31b	30b	31b
1	17.73	272.7	16.6	2.90	0.038	0.0106	0.00014
2	10.74	288.4	17.3	3.24	0.092	0.0112	0.00032
3	10.74	339.2	38.8	4.04	0.126	0.0119	0.00037

[a] Irradiated at 366 nm. [b] Analyzed for by HPLC.

Table XVI. Crystalline-State Quantum Yield Summary for 4,4-Di-1-naphthylcyclohexenone (29c)

run no.	reactant, mmol × 10^3	light abs,[a] μEinsteins	product,[b] mmol × 10^3	% conv	quantum yield 30
1	22.99	168.4	0.974	4.24	0.00578
2	10.92	103.5	0.567	5.19	0.00547
3	13.22	233.5	1.221	9.24	0.00523

[a] Irradiated at 366 nm. [b] Analyzed for by HPLC.

Table XVII. Conditions Employed in the Crystallization-State Quantum Yield Determination for 1,1,5,5-Tetraphenyl-3,3-dimethyl-4-penten-5-ol (42)

run no.	reactant, mmol × 10^3	light abs,[a] μEinsteins	% conv	photoproduct,[b] mmol × 10^3		quantum yield	
				45	44	45	44
1	13.62	60.87	6.08	0.3460	0.4814	0.00568	0.00791
2	18.63	102.6	7.29	0.6008	0.7575	0.00586	0.00739
3	17.20	122.3	9.52	0.7160	0.9208	0.00586	0.00753

[a] Irradiated at 302 nm. [b] Analyzed for by ^{1}H NMR.

suspension of 3,3-dimethyl-1,1,5,5-tetraphenyl-1,4-pentanediol in 30 mL of 6 M HCl was stirred for 16 h. Extraction with ether followed by basic workup[27] yielded 0.058 g of a colorless oil. The oil was subjected to preparative TLC eluted twice with hexane to yield 0.055 g of the tetrahydrofuran. Recrystallization from hexane yielded 0.051 g (0.122 mmol) (88.4%) of 3,3-dimethyl-2-(diphenylmethyl)-5,5-diphenyltetrahydrofuran.

General Procedure for Single-Crystal X-ray Structure Determination. X-ray diffraction data were collected on either a Nicolet (Syntex) P-$\bar{1}$ or P3/F diffractometer for single crystals of each compound. Unit cell parameters were determined by least-squares refinement of 25 reflections. Data were collected with 3 check reflections monitored after every 97 reflections. Data having $F < 3\sigma(F)$ were rejected. Lorentz and polarization corrections were applied, and each structure was solved under the appropriate space group symmetry by direct methods using SHELXS86.[30] Hydrogen atoms were located by difference Fourier synthesis, and full-matrix least-squares refinement was carried out employing anisotropic thermal parameters for all non-hydrogen atoms and isotropic thermal parameters for all hydrogen atoms. The results of the structure determinations and parameters for each compound are summarized in Tables V–X. Final molecular coordinates, geometries, and ORTEP drawings for each compound are given in the Supplementary Material.

General Procedure for Polycrystalline X-ray Diffraction. All polycrystalline X-ray diffraction patterns were measured on a Nicolet (Syntex) 12/V polycrystalline diffractometer equipped with a Cu Kα source. Samples measured were similar to those used for exploratory photolysis. The measured diffraction patterns were then compared with the patterns calculated XPOW[31] using the single-crystal data.

General Procedure for Quantum Yield Measurements. All quantum yields were determined with use of a microoptical bench[32] equipped with an Osram 200-W high-pressure mercury lamp and a Bausch and Lomb Model 33-86-79 monochrometer. The monochrometer entrance and exit slits were set to 5.4 and 3.0 mm, respectively, giving a 21.8 nm band pass at peak half-height. Light output was measured by using digital electronic actinometry[33] which was calibrated before and after each run with potassium ferrioxalate chemical actinometer.[18]

General Procedure for Solution Quantum Yields. All solution runs were made in 40 mL of the appropriate solvent (benzene or acetonitrile), the concentration of the reactant adjusted to absorb >99% of the incident light. The solutions were purged with deoxygenated and dried nitrogen[29] for 1 h prior to and during the photolysis. After photolysis, the solutions were concentrated in vacuo and photoproducts were analyzed by 200-MHz ^{1}H NMR with 4,4′-dimethoxybenzophenone as an internal standard.

The conditions employed in the photolysis, the ^{1}H NMR results, and the resulting quantum yields for each compound are summarized in Tables XI–XIII. The final quantum yields for each compound from extrapolation to zero percent conversion are given in Table II in the Results Section.

General Procedure for Solid-State Quantum Yields. All crystalline solid-state quantum yield runs were made with the appropriate amount of sample placed between two quartz plates (1 × 1.8 cm). The sample holder was then placed into the photolysis cell (see Figure 1 in the Discussion Section) against the back plate. The inner cavity of the photolysis cell was 11 cm deep with a diameter of 2 cm. Assuming random scattering, less than 3% of the light is expected to be reflected out the front of the cell. In practice, replacing the organic solid with powdered quartz results in less than 4% reflected out the front of the cell. The space around the sample was purged with deoxygenated and dried nitrogen[29] during the photolysis, and 93 mL of potassium ferrioxalate actinometer solution was placed in the surrounding jacket.[34] After the photolysis, the photoproducts were analyzed by either analytical HPLC[27] or ^{1}H NMR with 4,4′-dimethoxybenzophenone as an internal standard. The amount of light scattered by the sample was estimated by the amount of light absorbed by the potassium ferrioxalate actinometer in the surrounding jacket.

The conditions employed in the photolysis, the ^{1}H NMR results, and the resulting quantum yields for each compound are summarized in Tables XIV–XVII. The final quantum yields for each compound from extrapolation to zero percent conversion are given in Table II in the Results Section.

The crystalline-state quantum yield for 4,5,5-triphenylcyclohexenone (35) was estimated to be 0.000 03 for the appearance of *endo*-4,4,6-triphenylbicyclo[3.1.0]hexan-2-one from an extended photolysis run at 366 nm of 61.4 h (1.437 mEinsteins) on 13.5 mg (0.0416 mmol) of cyclohexenone 35. Analysis by analytical HPLC yielded 0.000 042 mmol (0.1%) of the endo-bicyclic ketone 39.

The crystalline-state quantum yield for 3-methyl-3-(2,2-dicyanovinyl)-1,1,5,5-tetraphenyl-1,4-pentadiene (5) was estimated to be 0.0005 for the appearance of 1-methyl-3,3,4,4-tetraphenyl-5-(2,2-dicyanovinyl)-1-cyclopentene from an extended photolysis run at 313 nm of 120 h (0.329 mEinstein) on 5.5 mg (0.0119 mmol) of the triene. Analysis by ^{1}H NMR revealed 0.000 262 mmol (2.2%) of the vinylcyclopentene 28.

Molecular Mechanics Calculations. Molecular mechanics calculations were performed with MM2 or MMP2.[35] Where torsional or bending constants were not available, constants approximating them were employed. For diradical species in which an aryl or vinyl group is half migrated, the spiro system is treated as a cyclopropane ring, and the odd-electron centers are treated as sp^2 carbons.

General Procedure for Geometry Analysis. Geometry analysis was performed with MACROMODEL[23] running on an Evans and Sutherland PS300 graphics terminal. Superimpositions were accomplished with the flexible superimposition routine based on the method of Kabsch.[36] Volumes were calculated with use of a modified version of VOLUME from the TRIBBLE package.[25] The volume program calculates the volume of a molecule by placing the molecule in a three-dimensional box of a known volume and generating a large number of random points within the box. The fraction of the points that are within the van der Waals radii of any atom in the molecule is the fraction of the volume of the box displaced

(33) Zimmerman, H. E.; Cutler, T. P.; Fitzgerald, V. R.; Weight, T. J. *Mol. Photochem.* **1977**, *8*, 379–385.

(34) The ferrioxalate solution was replaced periodically with fresh solution when necessitated by long irradiation times.

(35) Allinger, N. L.; Flanagan, H. L. *J. Comput. Chem.* **1983**, *4*, 399–403.

(36) (a) Kabsch, W. *Acta Crystallogr.* **1978**, *A34*, 827–828. (b) Kabsch, W. *Acta Crystallogr.* **1976**, *A32*, 922–923.

(37) Kitaigorodsky, A. I. *Molecular Crystals and Molecules*; Academic Press: New York, 1973.

by the molecule. The program was modified to allow a variable-point density and averaging of a series of volume calculations. The point density used and the number of averaged calculations gave a reproducibility better than ±1%. The van der Waals radii used were those reported by Kitaigorodsky[37] derived from X-ray crystallographic data.

Acknowledgment. Support of this research by the National Science Foundation and NIH Grant GM07487 is gratefully acknowledged. The synthetic portions were supported by the National Institutes of Health while the mechanistic aspects were supported by NSF.

Supplementary Material Available: ORTEP drawings and tables of positional parameters, interatomic distances, bond angles, anisotropic temperature factors, and isotropic temperature factors for 2,2-dicyano-5,5-dimethyl-3,3-diphenylbicyclo[2.1.0]pentane, **1-5**, **17**, **23**, **24c**, **26**, **25**, **28**, **29a**, **29b**, **29c**, **33**, **35**, **39**, **40**, and **42** (105 pages). Ordering information is given on any current masthead page.

Preparation of *tert*-Butyl-Capped Polyenes Containing up to 15 Double Bonds

Konrad Knoll and Richard R. Schrock*

Contribution from the Department of Chemistry 6-331, Massachusetts Institute of Technology, Cambridge, Massachusetts 02139. *Received February 28, 1989*

Abstract: 7,8-Bis(trifluoromethyl)tricyclo[4.2.2.0^{2,5}]deca-3,7,9-triene (TCDT) can be ring-opened in a controlled manner by W(CH-*t*-Bu)(NAr)(O-*t*-Bu)$_2$ (Ar = 2,6-C$_6$H$_3$-*i*-Pr$_2$) to give living oligomers from which the metal can be removed in a Wittig-like reaction with pivaldehyde or 4,4-dimethyl-*trans*-2-pentenal. Heating the oligomer yields a distribution of *tert*-butyl-capped polyenes, (*t*-Bu)(CH=CH)$_n$(*t*-Bu), where *n* is odd if pivaldehyde is used in the cleavage reaction or even if 4,4-dimethyl-*trans*-2-pentenal is used. Mixtures of odd and even polyenes have been analyzed by reversed-phase HPLC methods, and those having as many as 13 double bonds have been isolated by column chromatography on silica gel under dinitrogen at −40 °C and characterized by ^{1}H and ^{13}C NMR and UV-vis studies. The 17-ene has been observed by HPLC. Polyenes containing more than 17 double bonds are relatively unstable under the reaction and subsequent isolation conditions; those containing between 11 and 15 double bonds decompose thermally progressively more readily. The initial isomer in the odd-ene series has largely the trans(cis,trans)$_x$ geometry as a result of stereospecific trans initiation, stereoselective trans propagation, stereospecific trans cleavage, and stereospecific cis retro-Diels-Alder reactions. The even-ene series is more complex since the Wittig-like reaction involving 4,4-dimethyl-*trans*-2-pentenal is not selective. UV-vis and ^{13}C and ^{1}H NMR data have been collected and analyzed in detail for the trans(cis,trans)$_x$ isomers for x = 1-5 (up to 11 double bonds) and for the odd and even all-trans forms containing up to nine double bonds. Extrapolation of a plot of the energy of the $^1B_u \leftarrow {}^1A_g(0-0)$ transition versus $1/n$ (for up to the 13-ene) predicts that the HOMO-LUMO gap will be 1.79-1.80 eV for an infinite *all-trans*-polyene; in carbon disulfide it will be 1.56 eV. For the trans(cis,trans)$_x$ forms the $^1B_u \leftarrow {}^1A_g(0-0)$ energy gap is predicted to be 1.95 eV for an infinite polyene in a mixture of acetonitrile, dichloromethane, and water (90:5:5). The ease of thermal cis-to-trans isomerization (ultimately to the all-trans form) correlates directly with chain length, isomerization to the all-trans form being especially facile for the 13-ene and beyond. The *all-trans*-polyenes are significantly less soluble than forms that contain one or more cis double bonds, although cross-linking cannot be ruled out as a contributor to insolubility for polyenes longer than the 13-ene. The retro-Diels-Alder reaction in the first unit away from the metal in living polyTCDT is accelerated 10 times relative to that in the second unit away from the metal. Heating polyTCDT gives living polyenes that are stable at 50 °C for 45 min in solution; no benzene is formed.

Conjugated polyene chains are important components of natural products[1] and are a key feature of polyacetylene.[2] Isoprenoid polyenes containing up to 19 double bonds in the backbone are known,[3] but no polyene having an unsubstituted backbone longer than a 10-ene appears to have been prepared.[4] Since evidence is accruing that relatively short conjugated sequences can sustain a soliton,[5] it would be of fundamental interest to prepare well-defined unsubstituted polyenes that contain 10-20 double bonds.

(1) (a) Birge, R. *Annu. Rev. Biophys. Bioeng.* **1981**, *10*, 315. (b) Honig, B. *Annu. Rev. Phys. Chem.* **1978**, *29*, 31. (c) Zechmeister, L. *Cis-trans Isomeric Carotenoids, Vitamins A and Arylpolyenes*; Springer: Wien, 1962. (d) For proceedings of the International Symposium on Carotenoids see: *Pure Appl. Chem.* **1985**, *57*; **1979**, *51*; **1976**, *47*; **1973**, *35*; **1969**, *20*; **1967**, *14*.

(2) (a) Chien, J. C. W. *Polyacetylene Chemistry, Physics and Material Science*; Academic Press: New York, 1984. (b) Skotheim, T. A., Ed. *Handbook of Conducting Polymers*; Marcel Dekker: New York, 1986. (c) Kuzmany, H., Mehring, M., Roth, S., Eds. *Electronic Properties of Conjugated Polymers*; Springer Series in Solid State Sciences; Springer: New York, 1988; Vol. 76. (d) Bowden, M J., Turner, S. R., Eds. Electronic and Photonic Applications of Polymers. *Adv. Chem. Ser.* **1988**, *218*. (f) Proceedings of the International Conference on the Physics and Chemistry of Low-Dimensional Synthetic Metals. *Synth. Met.* **1987**, *17*; *Mol. Cryst. Liq. Cryst.* **1985**, *117*, 118. (g) Wegner, G. *Angew. Chem., Int. Ed. Engl.* **1981**, *20*, 361. (h) Baughman, R., Bredas, J.; Chance, R. R.; Elsenbaumer, R. L.; Shacklette, L. W. *Chem. Rev.* **1982**, *82*, 209. (i) Simionescu, C. I.; Perec, V. *Prog. Polym. Sci.* **1982**, *8*, 133.

(3) β-Carotene, one of the longest and most important of the naturally occurring polyenes, is an 11-ene isoprenoid.[1] The longest synthetic isoprenoid is dodecapreno-β-carotene, a 19-ene, obtained by derivatizing natural isoprenoids; see: Karrer, P.; Eugstler, C. H. *Helv. Chim. Acta* **1951**, *34*, 1805.

(4) A number of reviews are available.[4a-c] The longest well-characterized polyenes containing an unsubstituted backbone are 10-enes.[4c] Longer polyenes (e.g., the diphenyl-capped 15-ene[4a]) have been claimed,[4a,f] but no data are available that would allow one to confirm that this material is not cross-linked. Di-*tert*-butyl-capped poly*enynes* containing up to 30 carbon atoms have been reported.[4g] The synthesis of polyenes with up to eight double bonds having functionalized aryl end groups has been reported.[4h,i] (a) Kuhn, R. *Angew. Chem.* **1937**, *34*, 703. (b) Yanovskaya, L. A. *Russ. Chem. Rev.* **1967**, *36*, 400. (c) Hudson, B. S.; Kohler, B. E.; Schulten, K. In *Excited States*; Lim, E. C., Ed.; Academic: New York, 1982. (d) Bohlmann, F.; Mannhardt, H.-J. *Chem. Ber.* **1956**, *89*, 1307. (e) Sondheimer, F.; Ben-Efraim, D. A.; Wolovsky, R. *J. Am. Chem. Soc.* **1961**, *83*, 1675. (f) Nayler, P.; Witing, M. C. *J. Chem. Soc.* **1955**, *3037*. (g) Wudl, F.; Bitler, S. P. *J. Am. Chem. Soc.* **1986**, *108*, 4685. (h) Spangler, C. W.; Nickel, E. G.; Hall, T. J. *Polym. Prepr. (Am. Chem. Soc., Div. Polym. Chem.)* **1987**, *28*, 219. (i) Spangler, C. W.; Sapochuk, L. S.; Struck, G. E.; Gates, B. E.; McCoy, R. K. *Ibid.* **1987**, *28*, 219.

0002-7863/89/1511-7989$01.50/0